

The ROCK Inhibitor Fasudil and Sertraline Share Morphological and Molecular Effects in the Hippocampus of Chronically Stressed Rats: Exploring Common Antidepressant Pathways by Network Pharmacology

Gonzalo García-Rojo,[▼] Ignacio Valenzuela Martínez,[▼] Felipe Aguayo, Mauricio Muñoz-Llanos, David Ramírez,* and Jenny L. Fiedler*



Cite This: *ACS Pharmacol. Transl. Sci.* 2025, 8, 1292–1312



Read Online

ACCESS |

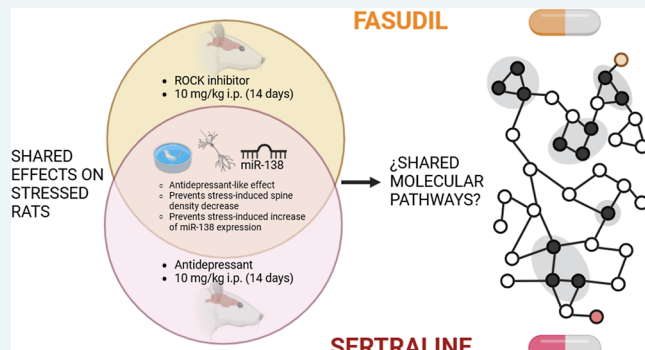
Metrics & More

Article Recommendations

Supporting Information

ABSTRACT: Despite the widespread use of selective serotonin reuptake inhibitors like sertraline, the intricate molecular mechanisms underlying major depression and the therapeutic efficacy of these treatments remain not fully elucidated. Building on our preliminary findings, this study investigates the antidepressant effects of fasudil, a Rho-associated protein kinase (ROCK) inhibitor typically utilized as a vasodilator and antispasmodic, and compares its effects with those of sertraline using a chronic restraint stress model in rats. Specifically, we examined the effects of chronic administration on dendritic spine density, key molecular survival pathways, and miRNA levels in the hippocampus. Adult male Sprague-Dawley rats were administered sertraline, fasudil (10 mg/kg/day), or saline over 14 days, with a subset experiencing daily restraint stress. Our findings demonstrate that both sertraline and fasudil effectively prevented stress-induced reductions in dendritic spine density and miR-138 levels in the rat hippocampus. Additionally, by employing a network pharmacology approach, we explored the converging molecular pathways influenced by both drugs, facilitating the identification of novel molecular targets and pathways implicated in the pathophysiology of depression and its treatment. Pharmacoinformatic analysis revealed common signaling cascades and critical proteins that may potentially underlie the observed pharmacological effects, contributing to a paradigm shift in understanding depression by integrating drug repurposing and network pharmacology, offering valuable insights into the underlying mechanisms of depression and the antidepressant effect from a new network-based paradigm rather than focusing solely on a single protein target.

KEYWORDS: sertraline, fasudil, miRNA, antidepressant, network pharmacology, depression



Depressive and anxiety disorders have emerged as the most disabling mental disorders, ranking among the leading causes of burden worldwide.¹ Despite the considerable impact of major depression, little is known about the precise molecular mechanisms associated with its etiology and how the antidepressants produce their therapeutic effect. Drugs like sertraline or fluoxetine, which are selective serotonin reuptake inhibitors (SSRI) antidepressants, have been used for decades and their prescription rates have significantly increased.² However, there is a considerable lag time between the blockage of serotonin transporter by these drugs and the onset of antidepressant effects (usually 3 to 8 weeks) evidenced as a reduction in clinical symptoms or severity.³ Thus, the described mechanism of antidepressants' action, specifically the increase in the concentration of monoamines in the synaptic cleft, is not sufficient to explain the pharmacological effects. Converging lines of evidence have shown

adaptive adjustments in several neuroplasticity-related mechanisms including variation in the gene expression, modification in synaptic biomarkers in diverse brain areas, and hippocampal neurogenesis.⁴ Therefore, a better understanding of the mechanisms underlying depressive disorders and antidepressant drug action is crucial to develop more effective and safer pharmacological treatments.

Genetic research has highlighted the heritability of depression and the interaction between genes and the

Received: November 23, 2024

Revised: February 26, 2025

Accepted: March 27, 2025

Published: April 3, 2025



Table 1. Summary of Sertraline and Fasudil Effects on Behavioral Tests

behavioral test	outcomes	restraint stress	sertraline	fasudil
forced swim test	depressive behavior and the efficacy of antidepressants	increase time spent in immobility compared to control (depressive-like behavior) in restraint stressed rats ^{9,23} and other models, such as social defeat stress ²⁵	the administration of sertraline prevents an increase in the time spent in immobility (indicative of anti-depressant-like behavior) in stressed animals and promotes an increase in swimming behavior ⁹	the administration of fasudil prevents an increase in the time spent in immobility (indicative of anti-depressant-like behavior) in stressed animals and promotes an increase in climbing behavior ²³
elevated plus maze	anxiety and the anxiogenic or anxiolytic effect	decrease on the open to total ratios (OTR) for entries and OTR for time, compared to control (anxiety behavior) ^{9,22}	administration of sertraline on control or stressed animals did not elicit anxiolytic or anxiogenic-like effects ⁹	administration of fasudil partially prevents the stress-induced decrease OTR and OTR for time, indicating an anxiolytic-like effect ²²
active avoidance conditioning	associative learning and memory	decrease of conditioned avoidance responses (CAR) and increase of escape failure (EF) ⁹	Sertraline administration on control animals reduces the CAR. However, in stressed animals, the drug prevents the reduction of CAR and increase of EF ⁹	fasudil administration prevents the decrease of CAR and increase of EF, on stressed animals ²²

environment as important factors in depression vulnerability,⁵ in which stress seems to play a significant role in the development of this complex psychiatric disorder.⁶ In fact, the prevalence of depression increased during the COVID-19 pandemic, likely due to elevated stress levels in the population.⁷ Animal models based on chronic stress protocols can emulate depressive-like behaviors in rodents, observable in behavioral tests, as well as findings at the anatomical and molecular levels that resemble those observed in humans.^{8–10} Similarly, these models are responsive to antidepressant drugs, as they can prevent and/or reverse the effects of stress.¹¹ One of the most reported findings both in humans and animal models of depression is the reduction in hippocampal volume.^{12,13} There are several factors that could contribute to hippocampal volume loss, including dendritic atrophy, spine density reduction of pyramidal neurons,^{10,14} and reduction in glial density.¹⁵ Additionally, a decrease in the activity of signaling pathways linked to neuroplasticity, neuron survival, and neurogenesis has been described,¹⁶ being the CREB/BCL-2 pathway crucial in the antidepressant drug actions and its dysregulation in depressive disorder.^{17–19} Moreover, molecular actors such as microRNAs (miRNAs) have been in the spotlight of depression etiology,²⁰ where these small non-coding RNAs play an important role in post-transcriptional gene regulation by controlling mRNA translation.²¹

We have previously reported that chronic administration of fasudil, a Rho-associated protein kinase (ROCK) inhibitor used as a vasodilator and antispasmodic, showed antidepressant-like effects in the forced swimming test (FST) similarly to sertraline.²² Thus, fasudil and sertraline prevent the restraint stress-induced increase in immobility time in rats during the FST.²³ Additionally, fasudil and sertraline prevent both stress-induced anxiety and the impairment of associative learning,²² which are behaviors related to hippocampal function (Table 1). Fasudil has been reported to exhibit an antidepressant-like effect not only in unstressed adolescent rodents²⁴ but also in other stress models.²⁵ Additionally, our findings indicate that fasudil prevents chronic restraint stress-induced dendritic spine loss in the rat hippocampus,²³ suggesting an important role in structural neuroplasticity.^{14,26} Interestingly, evidence has shown that miRNAs impact neuronal structural plasticity associated with dendritic spine density, modify their levels under chronic stress, and may play a significant role in the antidepressant effect of drugs.^{10,27} Thus, the identification of multiple targets of miRNAs introduces new levels of complexity to the current understanding in not only the stress response but also the antidepressant mechanisms and pathways involved.

Based on the aforementioned findings, fasudil emerges as a potential candidate for drug repurposing as an antidepressant, with a potential use for treatment of resistant depression, as suggested by an *in silico* approach.²⁸

Given the shared antidepressant-like effects of fasudil with the antidepressant sertraline, we explored whether spine density, molecular pathway CREB/BCL-2 related to cell survival, and miRNA levels in the hippocampus are specifically influenced by the chronic administration of each drug that may explain the broad actions in the rat chronic restraint stress model. Additionally, we evaluated the converging pathways of both drugs using network pharmacology, which may unveil novel molecular key players and pathways related to structural neuroplasticity. This study contributes to a paradigm shift in understanding depression and antidepressant mechanisms by integrating drug repurposing and network pharmacology strategies.

RESULTS AND DISCUSSION

This study compared the morphological and molecular effects in the hippocampus of rats treated with the SSRI antidepressant sertraline or the ROCK inhibitor fasudil, aiming to determine shared mechanisms/pathways that could explain the common antidepressant-like effect in the FST^{9,23} of these drugs, which differ in terms of their structure, as well as their currently described molecular targets and mechanisms.

Effect of Sertraline or Fasudil Treatment on Stress-Induced Reduction of Body Weight Gain. Chronic restraint stress is widely used to recapitulate depression phenotypes in rodents such as anhedonia, observed as a decrease in sucrose preference.^{8,10} Additionally, animals subjected to chronic stress exhibit an increase in the time spent in immobility in the FST.^{9,23} These behaviors can be prevented by the chronic administration of known antidepressants, thereby supporting the predictive validity of the model.⁸ It is widely reported that chronic stress models result in a decrease in weight gain.^{9,10,23} According to this, we registered the weight gain as a stress readout to corroborate the efficacy of the stress exposure protocol. During the days prior to drug administration and exposure to the stress protocol (−10 to day 0), the variation in weight gain between groups showed no differences (Figure 1). However, following the initiation of treatment, distinct patterns of weight gain emerged among the groups. A two-way ANOVA was performed, which showed a significant effect of time (days) ($F_{24, 625} = 479.9, p < 0.001$), treatments ($F_{5, 625} = 98.20, p < 0.001$), and the interaction of these factors ($F_{120, 625} = 5.594, p < 0.001$) (Figure 1A). Additionally, to analyze how sertraline or fasudil and stress impact the weight gain, a two-way ANOVA was

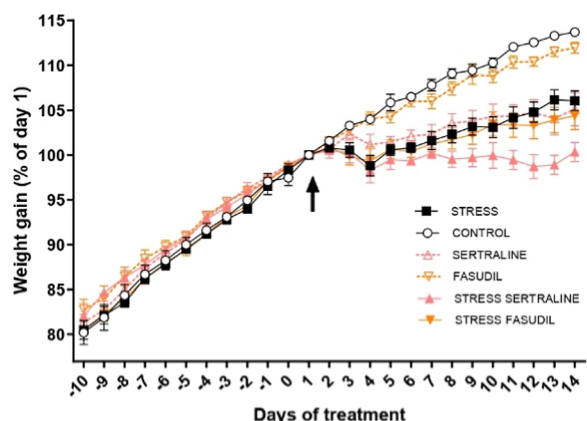
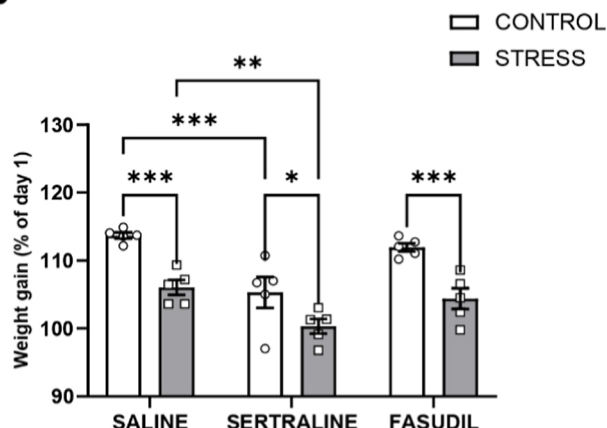
A**B**

Figure 1. Effect of stress and sertraline or fasudil treatment on body weight gain. (A) Plot represents mean \pm SEM of changes in body weight as a percentage of initial values for the control animals. Black arrows indicate the starting point of drug treatment and/or restraint stress protocol. (B) Variation of body weight at the end point of treatments (on day 14), representing the total percentage change in weight gain. Data were analyzed by two-way ANOVA followed by Fisher's LSD test. * p < 0.05; ** p < 0.01; *** p < 0.001. $N = 5$ for all conditions. Table S2 shows detailed statistical tests used.

conducted, focusing on the variations observed at the end point, i.e., in the last day of treatment. Stress ($F_{1, 24} = 38.89$, p < 0.001) and drug treatments ($F_{2, 24} = 15.53$, p < 0.001) but not the interaction of these factors showed a significant effect (Figure 1B). Post hoc analysis revealed that the STRESS group exhibited a reduction in weight gain of approximately 6% (p < 0.001) compared to the CONTROL group at the end of the 14 day treatment, and neither sertraline nor fasudil could prevent this effect. Fisher's LSD test analysis also indicated that the control group that received sertraline showed a significant decrease in weight gain of approximately 6%, compared to the control group (p < 0.001; CONTROL vs SERTRALINE). Furthermore, stressed animals treated with sertraline showed a lower increment in weight gain compared to the stress group (p < 0.05; STRESS vs STRESS SERTRALINE), suggesting an additive effect of sertraline and stress.

Our results revealed a similar weight gain rate in all animals in the days preceding stress application or drug administration, demonstrating a normal and comparable physiological state among all experimental animals. Subsequently, from day 1 of stress, stressed animals exhibited a significant decrease in weight gain, possibly mediated by reduced food intake and metabolic changes.²⁹ As for the action of the pharmacological agents used, it was observed that, unlike fasudil, sertraline caused a decrease in weight gain in both stressed and nonstressed animals. One possibility is that the animals treated with sertraline reduce their food intake. In agreement, it is well-documented that selective SSRIs may reduce appetite and consequently lead to a decrease in food consumption in rats through a serotonin-dependent mechanism,^{8,9,30} which is therefore an expected outcome for sertraline. In contrast, fasudil did not alter weight gain, which is consistent with our previous report.²³

Sertraline and Fasudil Prevent Stress-Induced CREB Dysregulation without Affecting BCL-2 Expression. The CREB/BCL-2 pathway has a crucial role not only in cell differentiation and survival but also in the structural and functional plasticity of neurons.¹⁹ This is particularly relevant considering the hippocampal volume reduction observed in depressive subjects and associated animal models.^{12,13} We evaluated the levels of proteins CREB, pSer133CREB, and BCL-2 to establish the impact of sertraline and fasudil treatments on this pathway. Representative Western blot bands are shown in Figure 1A, while uncropped blot images used for quantification are available in Figure S1 (Supporting Information). The two-way ANOVA of CREB protein levels show statistically significant interaction between stress and treatment effects ($F_{2, 24} = 9.263$, p < 0.01). Fisher's LSD post hoc analysis revealed an increase in CREB levels of control animals treated with sertraline (p < 0.01; CONTROL vs SERTRALINE) and stressed animals receiving saline (p < 0.05; CONTROL vs STRESS). Interestingly, although fasudil did not trigger any change in CREB levels of controls, both sertraline and fasudil prevented the stress-induced increase in CREB levels (p < 0.05) (Figure 2B). The increased CREB levels of control animals treated with sertraline are consistent with chronic administration of other SSRIs such as desipramine and fluoxetine.^{8,31} Additionally, in stressed animals, sertraline and fasudil prevented the stress-induced increase in CREB, showing a differential effect depending on the stress condition. The mechanism by which stress or antidepressants modify CREB protein levels is not fully described; it is believed that the effect might be mediated through their action on 5-HT or adrenergic receptors.³¹

CREB regulates important genes such as BCL-2 and BDNF, essential for neuronal functions.¹⁹ Serotonin can activate the MAPK pathway through the activation of its receptors (especially the 5-HT7 receptor) in hippocampal neurons.^{32,33} On the other hand, the activating phosphorylation of CREB (Ser133) has been described as an effect of antidepressants and proposed as a convergent point among various classes of these drugs.³⁴ However, when evaluating the levels of pCREB relative to actin, no changes were observed in any experimental group (Figure 2C), which could indicate that changes in the activation of this pathway are not an indispensable event in the antidepressant effect observed in the FST. We also analyzed the BCL-2 protein, recognized for its role in apoptosis regulation and cellular survival, with established connections to the antidepressant effect.^{35,36} Neither stress nor drug

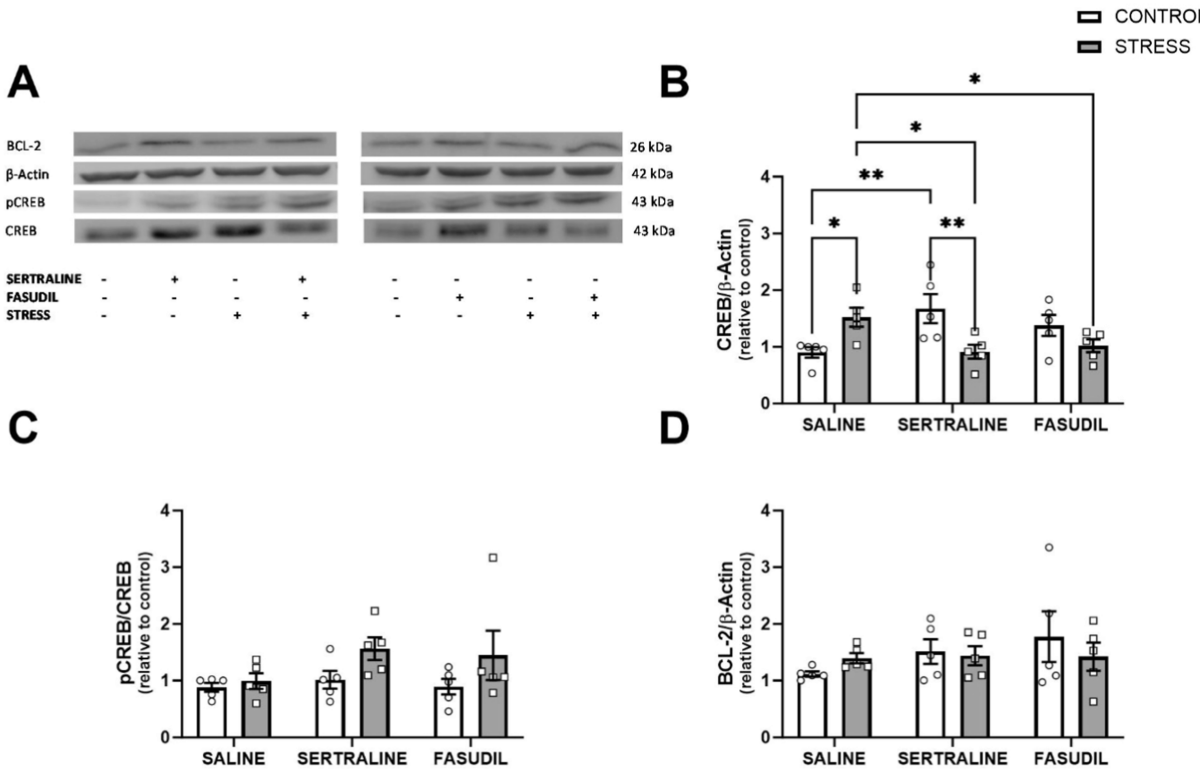


Figure 2. Effect of stress and sertraline or fasudil treatment on CREB/BCL-2 pathway protein levels in the rat hippocampus. (A) Representative immunoblots of analyzed proteins. The bar graphs (mean \pm S.E.M.) illustrate the impact of restraint stress and the treatments (sertraline or fasudil) in control (white bars) and stressed animals (gray bars), on (B) CREB, (C) pSer133CREB, and (D) BCL-2 protein levels relative to control, in whole hippocampal homogenates. CREB and BCL-2 were normalized using β -actin as the loading control, while pCREB were expressed as a ratio of phosphorylated/total protein. Data were analyzed by two-way ANOVA followed by Fisher's LSD test. * p < 0.05; ** p < 0.01. N = 5 for all conditions. Table S2 shows detailed statistical tests used.

treatments produced any effect on BCL-2 protein levels (Figure 2D).

These results indicate a greater impact of sertraline compared to fasudil on CREB protein levels, with both drugs preventing the stress-induced increase in CREB. However, the pCREB/CREB ratio and BCL-2 levels remained unchanged across all experimental conditions.

Both Sertraline and Fasudil Prevented the Chronic Stress-Induced Spine Density Decreases in Apical Dendrites of CA1 Pyramidal Neurons. The morphological alteration of neurons specifically dendritic atrophy and reduced spine density in pyramidal neurons^{10,14} is closely associated with depression-like behaviors in animal models, suggesting that changes in excitatory synapses may contribute to the symptoms of depression.¹⁴ Dendritic spines are considered a potential target for antidepressant-like effects, providing insights into the shared effects exhibited by fasudil and sertraline in behavioral tests. Therefore, the effect of stress, sertraline, and fasudil on the density of apical dendritic spines in CA1 hippocampal neurons was evaluated (Figure 3A). Two-way ANOVA indicated a main effect of stress ($F_{1, 21} = 10.80$, p < 0.01) but not of drug treatments; nonetheless a significant interaction was detected ($F_{2, 21} = 6.923$, p < 0.01). Fisher's LSD post hoc analysis revealed that stress produced a statistically significant decrease (p < 0.001; CONTROL vs STRESS) in dendritic spine density, an effect that was prevented by the administration of sertraline (p < 0.05; STRESS vs STRESS SERTRALINE) and fasudil (p < 0.01; STRESS vs STRESS FASUDIL) (Figure 3C). However, both

sertraline and fasudil did not alter the spine density in unstressed animals, indicating that the effect is determined probably by the state of the stress response. Similar results have been observed in control animals administered with amitriptyline³⁷ or fluoxetine³⁸ for 14 days. The decrease in hippocampal dendritic spines observed in stressed rats is consistent with increases in depressive-like behaviors, such as heightened immobility time in the FST, as reported in other studies.^{10,39} Additionally, the reduction in spine density has been associated with anxiety behaviors and associative learning (Table 1),^{9,22} while associative memory formation increases dendritic spines in the CA1 area of the hippocampus.⁴⁰ Given that dendritic spines are structures where synaptic connections may occur, it is evident that changes in the proportion of immature and mature dendritic spines and their density may be closely associated with behavioral performance. Furthermore, antidepressants have been demonstrated to reverse some of these structural changes, suggesting that alterations in dendritic spines and plasticity at excitatory synapses contribute to depression symptoms.¹⁴ In this context, tricyclic antidepressants like amitriptyline,³⁷ imipramine,⁴¹ desipramine,³⁹ and fluoxetine⁴² have been shown to prevent or reverse the reduction of dendritic spines in the CA1 area of the hippocampus. In our study, we demonstrated that sertraline prevented the chronic restraint stress-induced spine density decrease in apical dendrites of CA1 hippocampal pyramidal neurons. Similarly, our previous research showed that chronic administration of fasudil also prevented dendritic spine reduction in chronically stressed animals,²³ which is confirmed

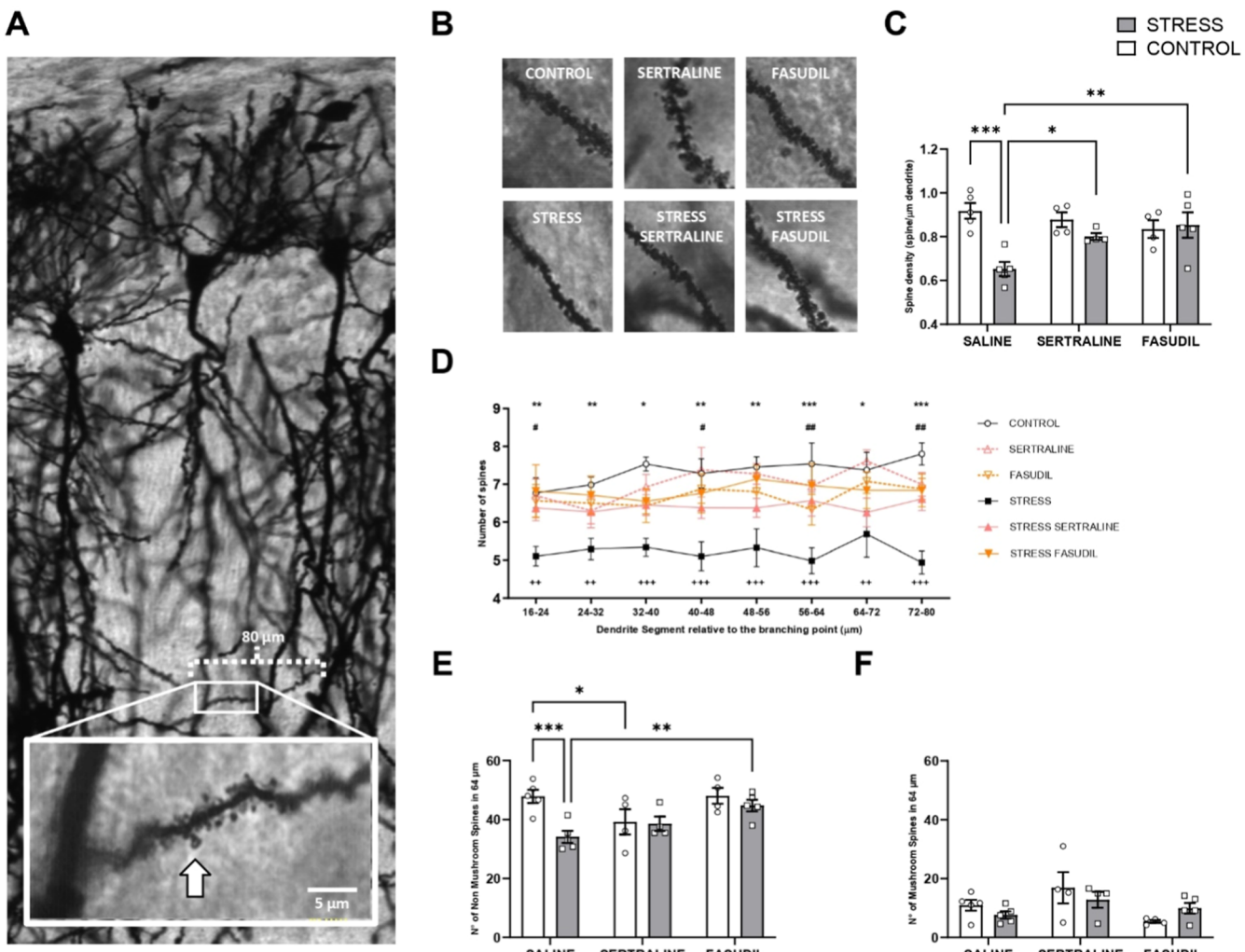


Figure 3. Effect of stress and sertraline or fasudil treatment on spine density and morphology in apical dendrites of CA1 hippocampal pyramidal neurons. (A) A representative isolated Golgi-stained pyramidal neuron from the CA1 hippocampal region in the *stratum radiatum* area is presented. The segment of the dendrite used for spine counting was located 16 μm from the initial branching point and extended up to 80 μm . In the magnified view, various dendritic spine types are observed: "Mushroom spines" (white arrow) were identified when their head diameter exceeded 0.6 μm , while the remaining spines (filopodia, stubby spines, and other protrusions) were classified as "non-mushroom spines". (B) Representative dendrite segments for each experimental condition studied. (C) The graph (mean \pm S.E.M.) shows the effect of the restraint stress and the treatments (sertraline or fasudil) in control (white bars) and stressed animals (gray bars), on the spine density in a 64 μm segment, expressed as the number of spines per μm of dendrite. Data were analyzed by two-way ANOVA followed by Fisher's LSD test. * p < 0.05; ** p < 0.01; *** p < 0.001. (D) Segmental analysis of the spine density (mean \pm S.E.M.) along a secondary dendrite, every 8 μm segments starting at 16 μm from the branching point. Data were analyzed by two-way ANOVA followed by Fisher's LSD test. CONTROL vs STRESS (* p < 0.05; ** p < 0.01; *** p < 0.001); STRESS vs STRESS SERTRALINE (# p < 0.05; ## p < 0.01); STRESS vs STRESS FASUDIL (* p < 0.05; ** p < 0.01; *** p < 0.001). (E) The bar graphs (mean \pm S.E.M.) illustrate the effect of the restraint stress and the treatments (sertraline or fasudil) in control (white bars) and stressed animals (gray bars), on the number of "non-mushroom spines" and (F) "mushroom spines" in a 64 μm dendrite segment. Data were analyzed by two-way ANOVA followed by Fisher's LSD test (* p < 0.05; ** p < 0.01; *** p < 0.001). (CONTROL N = 5, STRESS N = 5, SERTRALINE N = 4, FASUDIL N = 4, STRESS SERTRALINE N = 5, STRESS FASUDIL N = 5). Table S2 shows detailed statistical tests used.

in this study and constitutes a shared effect with sertraline and other novel drugs in depression treatment, such as the multimodal antidepressant vortioxetine, have also been found to influence hippocampal morphology, with reported increases in dendritic spine density in CA1,³⁸ similar to electroconvulsive therapy⁴³ and promising antidepressant agents like ketamine.⁴⁴ This convergence of effects on hippocampal dendritic spines by a variety of agents and treatments used for major depression indicates a clear relationship between this pathology and its treatment with dendritic spine density and remodeling.

To assess whether the preventive effect on the reduction of dendritic spine density induced by stress occurs in areas closer to the initial portion of the secondary dendrite or at more distal locations, an analysis was performed on the number of spines within 8 μm segments starting at 16 μm from the initial branching point. The two-way ANOVA (Figure 3D) showed a significant effect of treatment ($F_{5,168} = 29.20$, p < 0.001) but not of distance or the interaction between these factors. Subsequent post hoc analysis showed that stress reduced spine density along the dendrite compared to the control. However, the preventive effect of sertraline on dendritic spine loss of stressed animals (STRESS SERTRALINE vs STRESS) was

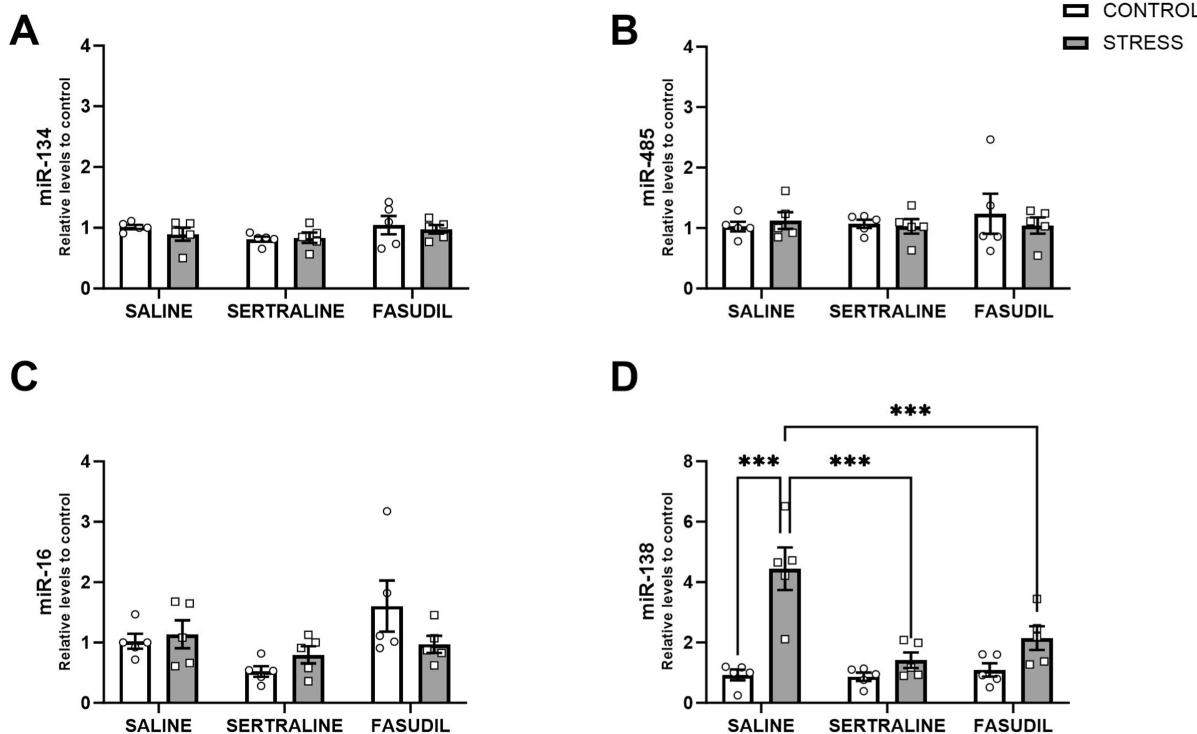


Figure 4. Effect of stress and sertraline or fasudil treatment on miR-16, miR-134, miR-138, and miR-485 levels in the rat hippocampus. The bar graphs (mean \pm S.E.M.) illustrate the effect of restraint stress and the treatments (sertraline or fasudil) in control (white bars) and stressed animals (gray bars), on (A) miR-134, (B) miR-485, (C) miR-16, and (D) miR-138 levels expressed as relative quantity compared to the CONTROL and normalized to SNORD95. Data were analyzed by two-way ANOVA followed by Fisher's LSD test (**p < 0.001). N = 5 for all conditions. Table S2 shows detailed statistical tests used.

exerted in determined segments of the dendrite (segments 16 to 24, 40 to 48, 56 to 64, and 72 to 80 μm). Fasudil, on the other hand, presented statistically significant preventive effects (STRESS FASUDIL vs STRESS) in every analyzed dendritic segment (Figure 3D). Thus, both drugs can prevent restraint stress-induced dendritic spine loss, but they exert their effects differentially along the CA1 of apical dendrites. This result may evidence differential molecular mechanisms of these drugs on dendritic spine density.

Sertraline and Fasudil Prevent Dendritic Spine Loss Differentially According to Their Morphological Features. Dendritic spines exhibit a variety of shapes, such as filopodia, stubby, cup-shaped, or mushroom-shaped, with the latter being crucial for synaptic connections.⁴⁵ Furthermore, we assessed spine types to establish potential differences in how sertraline and fasudil prevent dendritic spine reduction. To evaluate differential effects depending on spine morphology, we determined the number of mushroom-shaped dendritic spines and the rest of the spine types (nonmushroom-shaped spines) in the 64 μm analyzed dendrite segment (Figure 3E/F). On nonmushroom spines, analysis indicated a significant main effect of stress ($F_{1, 21} = 7.524, p < 0.05$), treatment ($F_{2, 21} = 4.192, p < 0.05$), and the interaction of these factors ($F_{2, 21} = 3.612, p < 0.05$). Post hoc tests revealed that the reduction in dendritic spine density induced by restraint stress occurred predominantly in nonmushroom spines ($p < 0.05$; CONTROL vs STRESS), reinforcing the idea that these “immature” spines are more sensitive to stress. Fasudil treatment in stressed animals prevented the reduction mainly in nonmushroom spines ($p < 0.05$; STRESS vs STRESS FASUDIL) (Figure 3E). In the case of sertraline, the role of

immature or nonmushroom spines alone in mitigating stress effects is not fully explanatory. For mushroom-type spines, a two-way ANOVA analysis showed a significant effect of treatment ($F_{2, 21} = 4.160, p < 0.05$). However, post hoc tests did not uncover any differences between groups.

Fasudil primarily acts on immature spines, like the action of another ROCK inhibitor, Y-27632, in primary hippocampal neuron cultures,^{19,46} suggesting the involvement of the ROCK protein in dendritic spine modification. Our previous findings demonstrate that the effects of stress and fasudil on dendritic spine density are related to the activation or inhibition of ROCK (determined by phosphorylation levels of MYPT1),²³ reinforcing the idea that ROCK has an active participation in hippocampal morphological changes. Altogether, these results suggest that the prevention of the decrease in the hippocampal dendritic spine density does not necessarily depend on serotonin reuptake inhibition or ROCK inhibition, given the known mechanisms for both drugs.

Both Sertraline and Fasudil Prevented the Chronic Restraint Stress-Induced Increase in miR-138 Levels. It has been reported that stress can alter the levels of numerous miRNAs in stress-sensitive brain regions such as the hippocampus and amygdala.⁴⁷ Several miRNAs have been linked to changes in dendritic density and morphology.⁴⁸ Recent studies also revealed interactions between miRNAs and ERK cascades, including CREB,⁴⁹ suggesting their potential role as significant contributors to the antidepressant effect. For instance, miR-134, found in dendritic spines, has been shown to decrease in response to immobilization stress.⁴⁷ Moreover, the CREB transcript is a validated target for miR-134⁵⁰ and a potential target for miR-485. Additionally, miR-16 has been associated

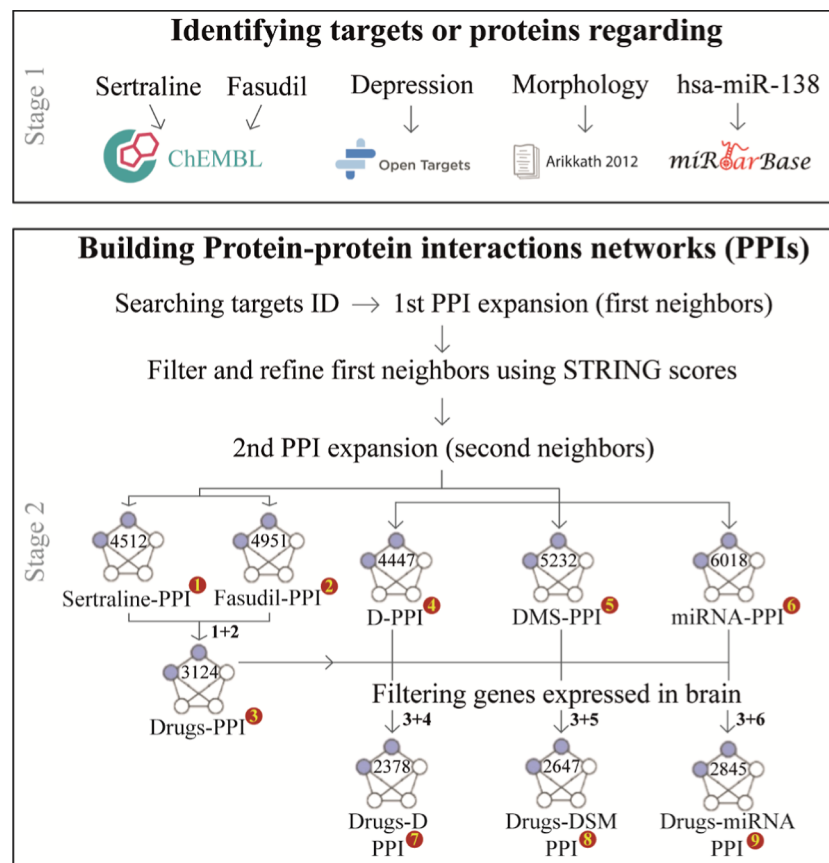


Figure 5. Construction of PPI networks. The figure illustrates the sequential process to build the PPI networks studied in this work, beginning with the identification of relevant targets and proteins related to sertraline, fasudil, depression (D), dendritic spine morphology (DSM), and hsa-miR-138 using various sources/databases (stage 1). These identified targets were then used to construct individual networks up to the second shell (second PPI expansion), followed by merging and filtering steps to obtain the final networks (PPI-7, PPI-8, and PPI-9) (stage 2). Further details on each step can be found in the Methods section. The red circles correspond to the ID numbering also shown in Table 2, and the number of nodes in each network is indicated within the network.

with the mechanism of the antidepressant fluoxetine³⁵ and our findings indicate that chronic restraint stress can elevate miR-138 levels in the hippocampus.¹⁰ In this study, we analyzed by two-way ANOVA the levels of miR-134, miR-485, miR-16, and miR-138 in a whole hippocampal homogenate (Figure 4). In contrast to miR-134 and miR-485, we observed a significant treatment effect ($F_{2, 24} = 4.179, p < 0.05$) on miR-16 levels; however, post hoc analysis did not identify any significant differences among the groups. In contrast, miR-138 levels exhibited a significant effect of stress ($F_{1, 24} = 32.09, p < 0.001$), treatment ($F_{2, 24} = 9.178, p < 0.01$), and the interaction of these factors ($F_{2, 24} = 9.267, p < 0.01$). Fisher's LSD post hoc analysis demonstrated that chronic stress significantly increased miR-138 levels ($p < 0.001$), with the stress-induced change being approximately four times higher than the control levels. Notably, this increase in miR-138 levels due to stress was effectively prevented by both sertraline ($p < 0.001$; STRESS vs STRESS SERTRALINE) and fasudil ($p < 0.001$; STRESS vs STRESS FASUDIL) (Figure 4D).

In this study, we corroborated the stress-induced increase in miR-138 hippocampal levels, and interestingly, both sertraline and fasudil prevented the miRNA increase triggered by stress. Importantly, neither sertraline nor fasudil altered miR-138 levels in nonstressed animals, suggesting that the responsiveness of this miRNA to both drugs in the rat hippocampus requires that the stress component miR-138 regulates dendritic

spine morphogenesis⁵¹ by influencing the translation of the APT1 transcript.⁵² APT1 is an enzyme that regulates the palmitoylation of several proteins that control dendritic spine volume, including the RhoA protein.⁵³ RhoA, a GTPase of the Rho family, acts through its effector, the ROCK kinase, and has been reported to induce spine shrinkage⁴⁸ (Figure S2A). ImmunoWestern blot analysis of APT1 on the whole hippocampal homogenate did not show significant changes among groups (Figure S2B,C, and Table S2), suggesting that morphological effects shared by sertraline and fasudil are not related to changes in APT1 levels. Moreover, it is important to consider that miR-138 may act by controlling gene expression through several mRNA targets, including validated and putative ones. Additionally, in the nucleus, miRNAs are pivotal regulators of gene expression, engaging in intricate interactions with various molecular entities. These small noncoding RNAs can associate with transcription factors, mRNAs, ncRNAs, and proteins, orchestrating a complex regulatory network that influences gene activity.⁵⁴ Thus, the multifaceted action of miRNAs permits control gene expression at multiple levels, impacting physiological signaling pathways in a complex way and protein–protein networks, which may influence cellular functioning.

In the context of our current and previously reported research, it is imperative to underscore the similar neuroprotective effects elicited by both sertraline and fasudil in the

Table 2. PPI Networks Constructed in This Study

ID	network name	description	# nodes	# edges	resulting of merge
1	sertraline-PPI	network centered in sertraline	4512	67,773	n/a
2	fasudil-PPI	network centered in fasudil	4951	67,048	n/a
3	drugs-PPI	merged network centered in both sertraline and fasudil	3124	26,298	1 + 2
4	D-PPI	depression-related proteins interaction network	4447	60,087	n/a
5	DSM-PPI	DSM proteins network	5232	68,474	n/a
6	miRNA-PPI	network centered on miRNA hsa-miR-138-5p targets	6018	75,088	n/a
7	drugs-D-PPI	merged network centered in both drugs and depression-related targets	2378	17,049	3 + 4
8	drugs-DSM-PPI	merged network centered in both drugs and DSM targets	2647	22,027	3 + 5
9	drugs-miRNA-PPI	merged network centered in both drugs and hsa-miR-138-5p targets	2845	22,830	3 + 6

hippocampus. These drugs have been demonstrated to ameliorate chronic stress-induced behavioral alterations and to preserve dendritic spine density within the CA1 hippocampal neurons as well as to regulate miR-138 levels. Notably, sertraline uniquely prevents stress-induced alterations in proteins pivotal to neuroprotection, a property not observed with fasudil, suggesting a differential mechanism of action, despite their similar therapeutic outcomes. Therefore, we propose a comprehensive investigation into these shared mechanisms to unravel the full spectrum of neuroprotective strategies employed by these agents in the context of stress-induced neuronal alterations. For this purpose, we conducted a complete network pharmacology analysis of drug–protein and protein–protein interactions (PPI) to elucidate the shared molecular pathways of these drugs. This approach extends beyond the mere identification of direct protein targets, encompassing the delineation of common signaling cascades that may underlie the observed pharmacological effects.⁵⁵

Sertraline and Fasudil Connect with Depression-, Dendritic Spine Morphology-, and miR-138-Related Proteins Evidenced by Network Pharmacology. The construction of protein–protein and drug–protein interaction networks (Figure 5) is a pivotal step in delineating the mechanistic pathways and potential targets of pharmacological agents. These networks not only shed light on the antidepressant effects of fasudil and conventional antidepressants such as sertraline but also provide insights into the molecular underpinnings of stress and depression. Integrating multiple therapeutic targets within these networks paves the way for the development of novel polypharmacological treatments, transcending the conventional one-target-one-drug paradigm.⁵⁵ Our study leverages these networks to discern the shared molecular interactions between sertraline and fasudil, aligning with proteins implicated in depression, dendritic spine morphology (DSM), and miR-138 (hsa-miR-138-5p) targets, thereby elucidating the common pathways that contribute to their observed therapeutic effects in the present study and those reported in the literature.

Table 2 provides a detailed summary of the designed PPI networks including the number of nodes (proteins) and edges (PPIs). In the merged network, common nodes are counted only once, resulting in a lower total number of nodes compared to the sum of the individual networks. This approach ensures comprehensive integration, combining all unique nodes and edges, and highlights shared proteins that interact with both drugs. Analyzing the final three networks (PPI-7, PPI-8, and PPI-9) revealed that sertraline and fasudil interact with distinct subsets of proteins associated with depression, DSM, and miR-138 targets. These interactions include both direct connections and indirect associations

mediated by neighboring nodes in critical areas related to both the observed and potential shared effects of these drugs.

Figure 6 illustrates the complex interplay between the drug targets and relevant proteins, emphasizing both direct and indirect interactions. Interestingly, both drugs have common targets, such as cytochrome P450 3A4 (CYP3A4) and potassium voltage-gated channel subfamily H member 2 (KCNH2). The latter protein, also known as human ether-à-go-go (hERG1), is a potassium channel predominantly expressed in the heart. In the brain, currents through hERG channel subunits play an important role in neuronal excitability and firing.⁵⁶ hERG has been linked to psychiatric disorders such as schizophrenia⁵⁷ and studies have found that its genetic variants or abnormal expression in the brain can alter neuronal activity and contribute to psychiatric symptoms.⁵⁸ Sertraline has an affinity for several cardiac ion channels, including hERG, blocking it as a result of this interaction. This relationship is commonly associated with adverse effects such as cardiac arrhythmias,⁵⁹ not only in this antidepressant but also with other SSRIs, as well as tricyclic and tetracyclic antidepressants that target this potassium channel.⁶⁰ For fasudil, there is a study indicating its affinity for hERG.⁶¹ However, its relationship with stress and depression, beyond cardiovascular effects, has not been well-explored in the literature. Therefore, it seems plausible and necessary to investigate its functionality in the central nervous system and the role it might play in antidepressant effects.

Additionally, it was discovered that there are proteins that are targets of the drugs and are also present among the target proteins of the PPI network under study. In the drugs-D-PPI network, the sodium-dependent dopamine transporter (SLC6A3) and the sodium-dependent serotonin transporter (SLC6A4) have been identified as key targets of sertraline and depression (Figure 6A). Meanwhile, cyclin-dependent kinase 5 (CDK5) is a target of fasudil and is also a protein associated with morphological changes in dendrites (Figure 6B). Furthermore, Rho-associated protein kinase 2 (ROCK2) is a target of both fasudil and hsa-miR-138-5p (Figure 6C), which is particularly interesting given the proven interaction between hsa-miR-138-5p and ROCK2.⁶² However, this interaction alone does not fully explain the observed effects at the experimental level in this study, as stressed animals exhibited an increase in miR-138, which coincided with a decrease in dendritic spine density. This suggests that the relationship with ROCK2 may be part of a more complex regulation or depend on the stress state of the animal.

Both Sertraline and Fasudil Share Pathways Related to Depression-, Dendritic Spine Morphology-, and miR-138-Related Proteins. Network-based analyses were conducted to elucidate the intersecting molecular pathways of

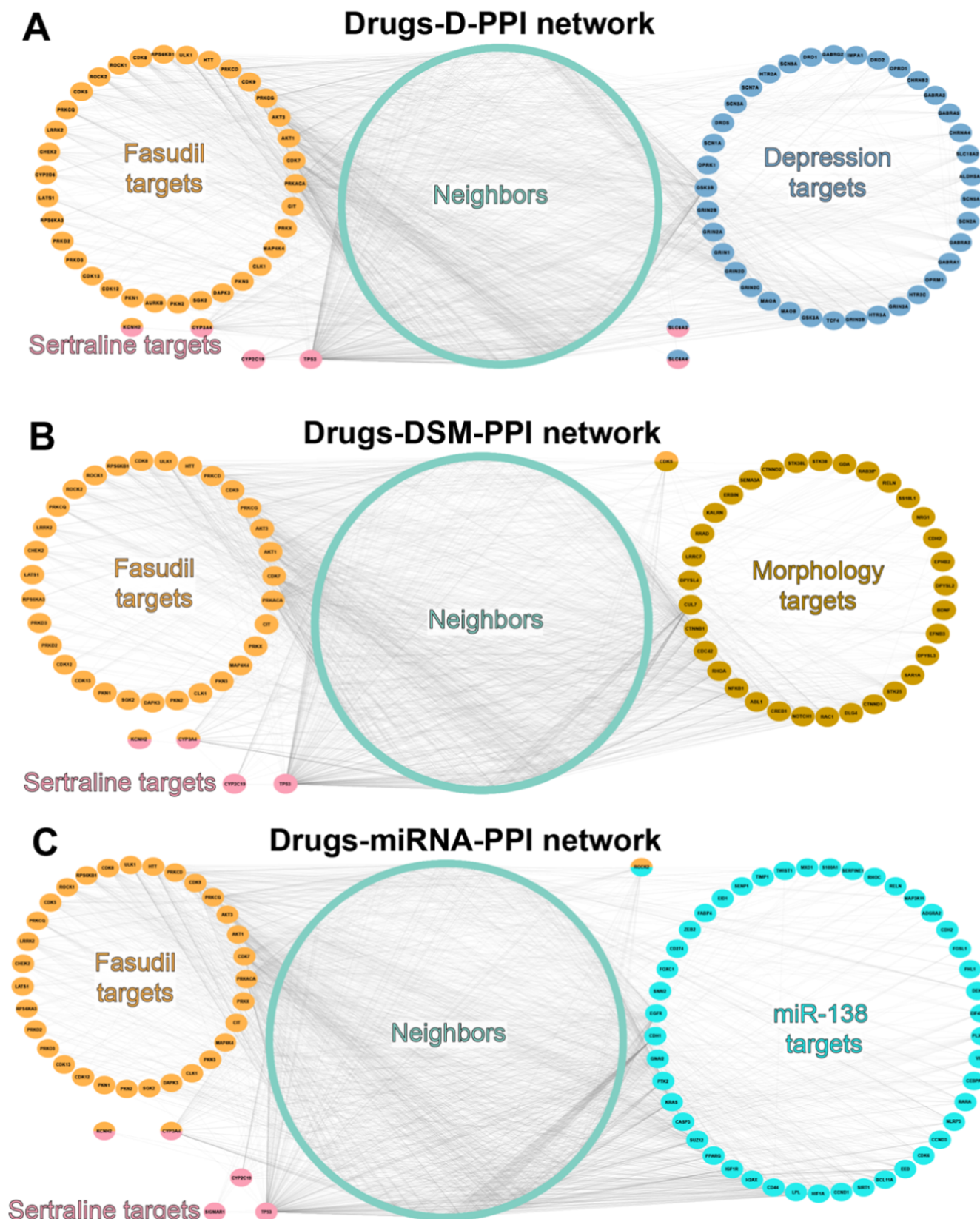


Figure 6. PPI networks. (A) Drugs-D-PPI depression-related targets are shown in blue. (B) Drugs-DSM-PPI. Proteins affecting dendritic morphology are shown in brown. (C) Drugs-miRNA-PPI. Hsa-miR-138-5p targets are shown in cyan. To enhance the visualization of how the first (targets) and second neighbors (green nodes) mediate PPIs between fasudil/sertraline targets and those related to depression/morphology/miR-138, connections among the neighbors are not displayed. Nodes with two features are colored with two colors, according to the above description.

Identifying the common paths into each PPI network

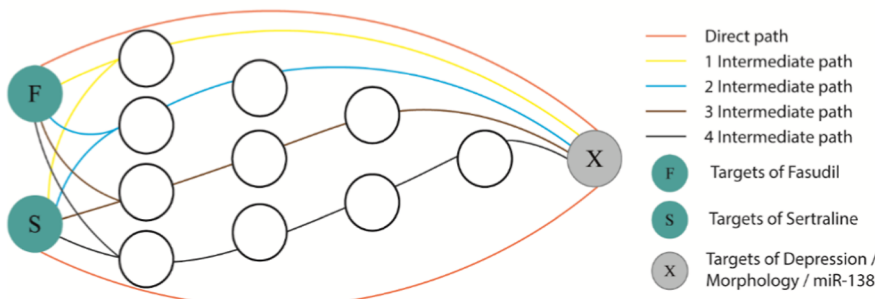


Figure 7. Common paths analysis. The figure illustrates the identification of common paths within each PPI network. The paths are categorized by their connection type: direct path and paths with 1 to 4 intermediates, each represented by different colored lines. “F” represents the targets of fasudil, “S” indicates the targets of sertraline, and “X” represents the targets associated with depression, morphology, or miR-138. The white circles represent intermediary nodes within the PPI networks, indicating how these intermediaries connect the primary targets. The analysis highlights potential shared pathways among the different targets.

sertraline and fasudil, with a focus on proteins implicated in depression, dendritic spine morphology, and miR-138 targets within the cerebral and hippocampal context (Figure 7). Our findings demonstrate that both pharmacological agents, via their respective targets, converge on multiple pathways that lead to proteins pivotal in the etiology of depression (refer to Figure S3).

In the networks related to depression (drugs-D-PPI) and miR-138 (drugs-miRNA-PPI), we observed a notable reduction in the number of shared pathways as the intermediary path length increased from three to four, with an approximately 3-fold reduction for the depression network (Figure 8A). This suggests a high degree of centralization and specificity within the key interactions of the depression network, highlighting potential critical nodes amenable to therapeutic targeting. A similar pattern emerged when the intermediary protein count within the depression network was examined (Figure 8B), indicating that the principal pathways are more direct and less intricate. Conversely, while the intermediary count escalated for the morphology and miR-138 networks, the overall protein count decreased (Figure 8C). This pattern suggests that these networks rely on a smaller set of crucial proteins that govern multiple pathways. Such a configuration may indicate a streamlined network architecture; however, it could also reflect reduced redundancy, potentially making the network more susceptible to disruptions.

Our comparative pathway analysis examined the common trajectories arising from the molecular targets of fasudil and sertraline, as shown in Figure S4. The findings indicate that fasudil engages in a broader array of pathways due to its larger set of identified targets. In contrast, sertraline, despite having fewer targets, exerts a significant influence on shared pathways, highlighting its importance in these molecular interactions. We identified key proteins mediating inputs and outputs (Figure 8D), with proteins from the MAPK pathway and Heat Shock Protein 90-alpha (HSP90AA1) emerging as crucial intermediaries across all three networks.

HSP90AA1, or Hsp90, is a highly conserved stress protein whose expression is induced by various stressors, including heat shock and inflammation. Recent evidence suggests a strong association between Hsp90 and depression, as it regulates the hypothalamic-pituitary-adrenal axis and neuroinflammation—two key mechanisms in depressive disorder.⁶³ Of note, Hsp90 participates in glucocorticoid receptor

maturity and is linked to neuroinflammation observed in depressed patients.^{63,64} Banach et al. (2017) found that neither sertraline nor venlafaxine significantly affected Hsp90 expression levels after 8 weeks of treatment in female depressed patients.⁶⁵ Nonetheless, the potential role of Hsp90 in depression remains promising, with the ongoing exploration of Hsp90 inhibitors for their therapeutic potential. Further investigation into the role of Hsp90 could yield valuable insights into developing novel antidepressant therapies targeting this chaperone. Moreover, the E3 ubiquitin-protein ligase (AMFR) and glutathione S-transferase P (GSTP-1) have been identified as significant within both the morphology and miR-138 networks (Figure 8D). While direct associations with depression are not established, their prominence in these shared pathways merits attention, as they may unveil novel correlates of the disorder. Glycogen synthase kinase-3 beta (GSK3 β) is highlighted as a crucial intermediary (Figure 8D) and a significant end point within the depression network, with multiple paths converging upon it (Figure 8E). GSK3 β also serves as a notable intermediary in several pathways leading to glycogen synthase kinase-3 alpha (GSK3 α). This is of particular interest given the association of elevated GSK3 β activity with chronic stress and depressive-like behaviors.⁶⁶ Our prior research demonstrated that fasudil effectively inhibits stress-induced phosphorylation of GSK3 β at Ser9,²² similar to the effects observed with long-term sertraline treatment in individuals with depression.⁶⁷ These findings underscore the therapeutic potential of GSK3 β as a target for novel depression treatments.

Path analysis revealed several proteins that could be relevant for the shared effects of the drugs studied and warrant further investigation. For instance, the inactivation of 5-hydroxytryptamine receptor 2A (HTR2A) has been shown to potentiate the effect of SSRI escitalopram in mice,⁶⁸ and this protein emerges as the output with the highest number of paths involved in three intermediary routes and ranks third in four-intermediary routes (Figure 8E). In the morphology and miR-138 networks, cyclic AMP-responsive element-binding protein 1 (CREB1), which was evaluated experimentally in this study (Figure 2D), and focal adhesion kinase 1 (PTK2) emerge as the only direct outputs (Figure 8E), while calcium-responsive transactivator (SS18L1) and eukaryotic translation initiation factor 4E-binding protein 1 (EIF4EBP1) have emerged as central nodes,

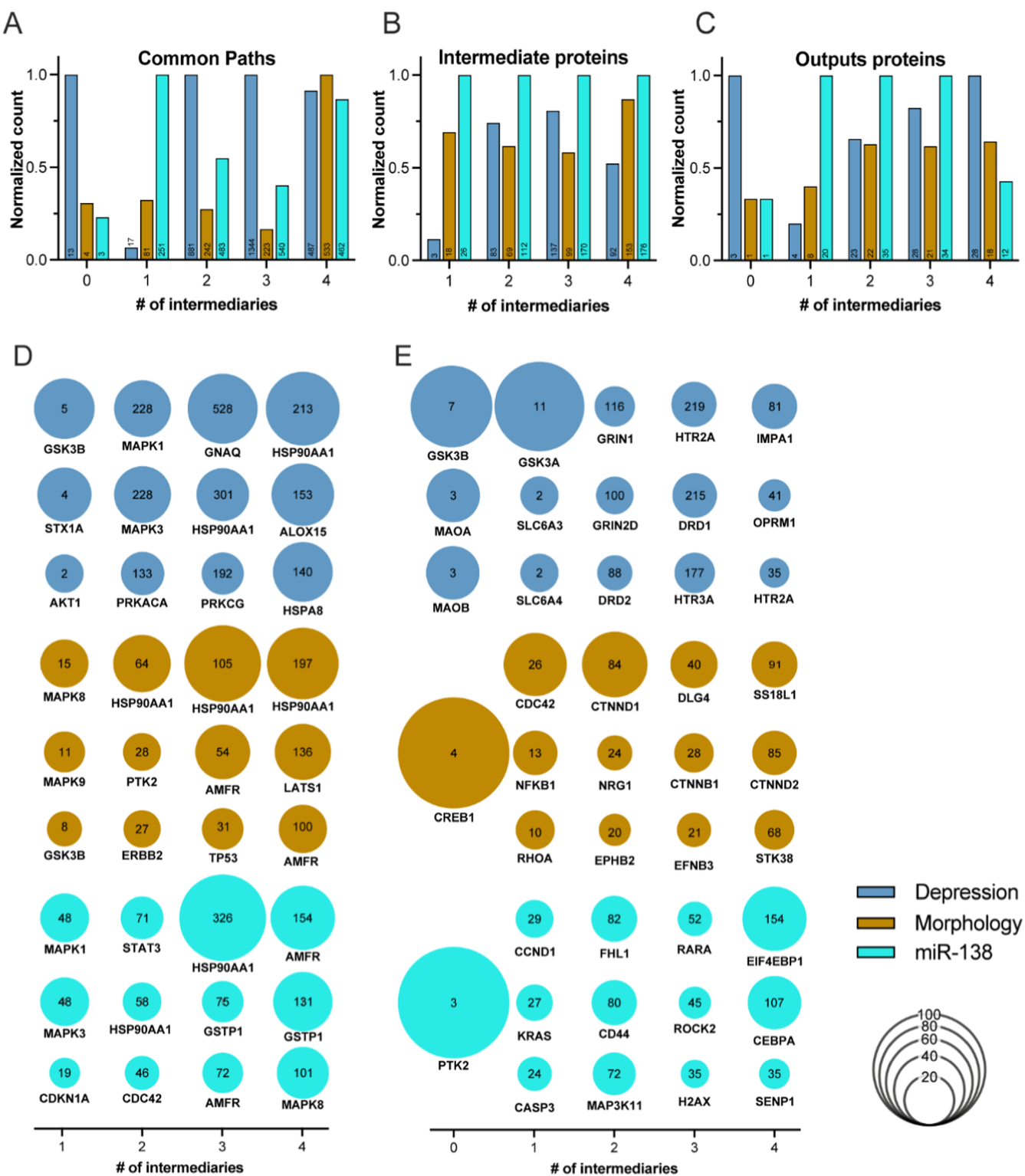


Figure 8. Path analysis of intermediates and outputs. (A) Bar chart displaying the shared paths between fasudil and sertraline, categorized by the number of intermediaries, for each respective network. (B) Bar chart displaying the proportion of proteins functioning as intermediates, categorized by the number of intermediaries involved, to each network. (C) Bar chart showing the proportion of outputs reached by the number of intermediaries for each network. Each bar in the charts has been normalized against the peak value across different networks for the corresponding number of intermediary proteins. The exact quantity of common paths, intermediates, and outputs is labeled directly on each bar. (D) Bubble chart showcasing intermediates with the most significant involvement in the paths. (E) Bubble chart highlighting the most frequently achieved outputs. The sizes of the bubbles indicate their percentage representation relative to the total number of paths, tailored for each specific intermediary count and network. Annotations within each bubble specify the precise frequency of each protein's involvement, indicating the number of paths in which the protein participates. In the bottom left corner, the color legends corresponding to the networks are displayed alongside the bubble sizes in relation to the percentage of paths.

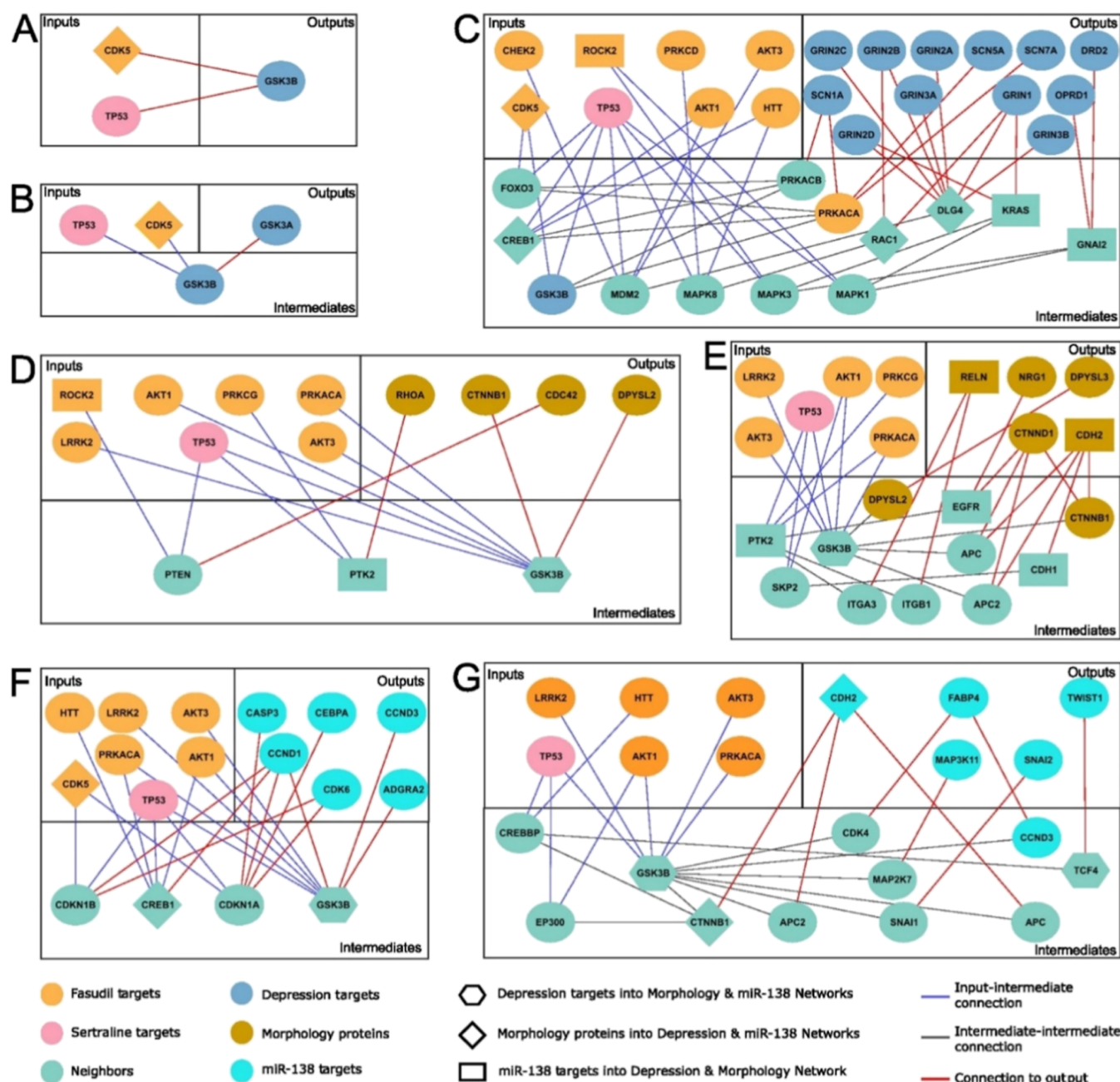


Figure 9. Path analysis subnetworks involving outputs from other networks. This analysis depicts the common paths between fasudil and sertraline toward proteins associated with depression, morphology, and miR-138, while also exploring their intersections and involvements with other networks. Diamond, hexagonal, and rectangular nodes denote proteins related to morphological changes, depression, and miR-138-5p targets, respectively. These nodes uniquely intersect with other networks, extending beyond their primary categories of analysis. The nodes display two distinct features and colors. Each panel is subdivided into inputs, intermediaries (where applicable), and outputs. (A) Direct common paths from fasudil and sertraline targets to depression targets. (B) Common paths mediated by an intermediary from fasudil and sertraline targets to depression targets. (C) Common paths involving two intermediaries from fasudil and sertraline targets to depression targets. Common paths involving miR-138 targets were filtered to include only those in which at least two of the miR-138 targets participate, for better visualization. (D) Common paths mediated by an intermediary from fasudil and sertraline targets to proteins related to dendritic morphology changes. (E) Common paths involving two intermediaries from fasudil and sertraline targets to proteins associated with dendritic morphological changes. Common paths involving miR-138 targets were filtered to include only those in which at least two of the miR-138 targets participate, for better visualization. (F) Common paths mediated by an intermediary from fasudil and sertraline targets to miR-138-5p targets. (G) Common paths involving morphology-related proteins were filtered to include only those in which at least two of morphology-related proteins participate, for better visualization.

receiving the most substantial number of common paths (Figure 8E).

Sertraline and Fasudil Reveal Common Routes across Distinct Depression-, Dendritic Spine Morphology-, and

miR-138-Related PPI Networks. After conducting path analyses for each network, we examined proteins of interest across PPI networks to assess their relevance in multiple contexts, suggesting potential key pathways in their shared

effects. Notably, within the depression network, we investigated the roles of proteins associated with morphology and targets of hsa-miR-138-5p. We found that CDK5, as previously mentioned, directly interacts with GSK3 β , similar to the interaction with cellular tumor antigen p53 (TP53) (Figure 9A).

The involvement of the tumor suppressor protein p53 in multiple signaling networks pertinent to depression and its response to antidepressants are particularly noteworthy. Recent research, including findings on a traditional Chinese herbal extract known for treating neurological disorders, has demonstrated its ability to regulate the P53/SLC7A11 signaling pathway, thereby inhibiting ferroptosis. In studies on poststroke depression (PSD), this herbal extract reduced stress-related elevations in p53 levels within the prefrontal cortex, which subsequently promoted neuroprotection by stabilizing key antioxidant systems such as GPX4.⁶⁹ These findings indicate that p53 may contribute not only to neurodegenerative processes but also to a critical role in neuroplasticity and stress-response mechanisms, which are closely linked to the pathophysiology of depression. This observation expands our understanding of p53's potential beyond its traditional roles in cell cycle regulation and apoptosis. p53 is involved in multiple molecular pathways that affect brain function and behavior, including those related to synaptic plasticity and neuronal survival, both of which are crucial for effective antidepressant responses. By modulation of ferroptosis, p53 demonstrates its broader involvement in maintaining neuronal health, underscoring its importance in preventing neuronal death and supporting synaptic function. Targeting p53 in therapeutic strategies may offer novel approaches to mitigate stress-induced neuronal damage, as observed in conditions like PSD and major depression.⁷⁰

Through the same interaction with GSK3 β , CDK5 acts as an input leading to GSK3 α (Figure 9B) and three members of the voltage-gated ion channel (VIC) superfamily: SCN1A, SCNSA, and SCN7A (Figure 9C). This cross-referencing approach was similarly applied to other networks to ensure a comprehensive examination of potential interactions and overlaps. The results detailed in Figure 9 clearly indicate that there is cross-participation of various proteins among the different networks common to sertraline and fasudil, which is more logical or expected for those related to depression and dendritic spine morphology, as their relationship is well-documented.¹⁴ Yet, this analysis provides a level of detail previously unachieved. More intriguing is the cross-linking of miR-138 target proteins with the depression and morphology PPI networks, which are also on the shared pathways of both drugs. This not only provides more consistent information about the role of miR-138 in processes that govern dendritic morphology and depression but also offers valuable insights about novel molecular actors and pathways that could be related to the antidepressant effect, which is a result far more valuable than merely repositioning fasudil as a new antidepressant drug.

Given the extensive data collected, we developed a ranking system based on pathing scores (PS) to identify the most influential proteins within the shared pathways. This scoring method assigned higher scores to proteins directly connected within the networks and progressively lower scores to those further along in the connection chain across at least two different networks, as detailed in Table 3. This systematic approach helped to highlight common routes across the

Table 3. Proteins with High PS in at Least 2 Out of 3 Analyses^a

string name	depression PS	morphology PS	miR-138 PS
TP53	0.351	1	1
GSK3B	0.740	0.129	0.117
HSP90AA1	0.044	0.116	0.140
KCNH2	0.037	0.058	0.066
KRAS	0.164	low score	0.587
MAPK1	0.180	low score	0.378
MAPK3	0.177	low score	0.352
CYP3A4	0.191	low score	0.028
ESR1	0.034	low score	0.069
HDAC1	0.042	low score	0.054
MAPK8	low score	0.195	0.089
MAPK9	low score	0.131	0.083
EP300	low score	0.089	0.098

^aLow score: did not exceed the cutoff score to be considered significant. The cutoff score is equivalent to the score of a direct interaction between input and output (see Methods).

distinct networks involved in depression-, dendritic spine morphology-, and miR-138-related protein interactions. The insights gained from this analysis could provide valuable directions for future research into these complex biological systems.

CONCLUSIONS

This study provides a deeper understanding of the antidepressant action achieved through pharmacological treatments, utilizing fasudil as a comparative tool against the well-known antidepressant, sertraline. Here, we have presented compelling evidence that sertraline and fasudil share effects in the stressed rat hippocampus at both the morphological (dendritic spine density) and molecular levels (proteins and miR-138). Our aim was to extend beyond mere morphological or molecular findings and further explore the potentially shared mechanisms and pathways of both drugs, employing a network pharmacology approach. The outcomes of these analyses revealed concordant pathways in PPIs targeting areas related to depression and morphology, including potential targets of miR-138, offering valuable insights into the underlying mechanisms of depression and the antidepressant effect from a new network-based paradigm rather than focusing solely on a single protein target.

METHODS

Animals. All animal procedures were conducted in strict accordance with internationally recognized ethical guidelines and were approved by the Ethics Committee of the Faculty of Chemical and Pharmaceutical Sciences, University of Chile (code CBE 2014-2). Animal care and handling followed the NIH Guide for the Care and Use of Laboratory Animals (NIH Publication, eighth Edition, 2011), and the study was conducted in alignment with ARRIVE (Animal Research: Reporting of In Vivo Experiments) guidelines and the principles of the 3Rs (replacement, reduction, and refinement).

Male adult Sprague-Dawley rats (250–280 g) were obtained from the institutional animal facility and housed in a temperature-controlled (22–23 °C) and humidity-regulated (55–65%) environment, with a 12:12 h light–dark cycle. Food (standard rat chow) and water were freely provided, except during stress procedures. To minimize handling-related stress,

animals underwent a 10 day habituation period, during which they were briefly handled daily for weighing. This procedure involved holding the animals by their bodies, placing them in a containment box on a scale, and allowing them to return to their home cage voluntarily. The housing environment was maintained as noise-free to reduce external stressors. The animals were monitored daily by a veterinarian, following the Morton and Griffiths (1985) protocol,⁷¹ which evaluates clinical signs of pain and distress, including body weight, coat condition, behavioral responses, and vital parameters. This system allowed for early detection of distress and guided human intervention when necessary. No animals exhibited severe distress or required euthanasia.

Restraint Stress and Pharmacological Treatment. The restraint stress procedure lasted 2.5 h per day for 14 consecutive days, specifically during the morning hours (9:00 AM to 12:00 PM) to control for potential circadian influences, such as fluctuations in corticosterone levels. During these sessions, animals were temporarily deprived of food and water and were returned to their home cages immediately after the procedure. This type of stress protocol is a less restrictive alternative to full immobilization methods, reducing unnecessary distress while maintaining the experimental reproducibility.

The conditions of the restraint stress protocol and fasudil and sertraline doses used were similar to previous studies to replicate and further explore underlying mechanisms regarding antidepressant-like effects.^{9,22,23} Thirty adult male Sprague-Dawley rats randomly received one of the following treatments: unstressed animals injected intraperitoneally every day for 14 days with (i) saline (0.9% NaCl; CONTROL group, $n = 5$), or (ii) 10 mg/kg sertraline (Saval Laboratories, Chile; SERTRALINE group, $n = 5$), or (iii) 10 mg/kg fasudil (LC Laboratories, Woburn, MA, USA; FASUDIL group, $n = 5$), or restraint-stressed groups injected intraperitoneally every day for 14 days with (iv) saline (0.9% NaCl; STRESS group, $n = 5$), or (v) 10 mg/kg sertraline (STRESS SERTRALINE group, $n = 5$), or (vi) 10 mg/kg fasudil (STRESS FASUDIL group, $n = 5$) 15 min prior to the restraint stress protocol in a Plexiglas tube as we described previously.⁸ The 10 mg/kg dose of fasudil was selected based on previous studies demonstrating its neuroprotective and behavioral antidepressant-like effects in rodents.^{23,72–74} Similarly, the 10 mg/kg dose of sertraline is widely used in preclinical models due to its good tolerability and efficacy in modulating depressive-like behaviors, as reported in previous studies, including our own laboratory's research.⁹ Twenty-four h after the last treatment, euthanasia was performed by decapitation without anesthesia to obtain either brain tissue to conduct morphological analyses or the hippocampus for protein and miRNA level determinations. This method was selected because it ensures a rapid loss of consciousness, prevents unnecessary suffering, and avoids biochemical alterations that could interfere with the study. The procedure was performed by trained personnel, ensuring compliance with ethical standards and minimizing potential suffering.

Golgi Staining and Evaluation of Dendritic Spine Density. After decapitation, the right brain hemisphere was used for Golgi staining, using the FD Rapid GolgiStain kit (FD Neuro Technologies, Baltimore, MD, USA), as we described.^{10,23} Protrusions that extend from the dendritic shaft, irrespective of their morphological characteristics, were considered as spines. A "mushroom" spine type was identified

when its head diameter exceeded 0.6 μm ; the remaining spines (filopodia, stubby, and other protrusions) were classified as "non-mushroom." Spines were counted in segments of 8 μm , starting at 16 μm from the origin of the branch, along 80 μm of the secondary dendrite. The number of spines at a given segment was then averaged using all of the neurons from the same animal (at least 6 neurons/animal), and these data were pooled with the mean of the other animals belonging to the same experimental group. The total number of spines corresponded to the sum of spines along a dendritic length of 64 μm .

Sample Processing and Homogenization for RNA and Protein Analysis. Frozen left hippocampus was homogenized in a glass-to-glass homogenizer in the presence of lysis buffer (50 mM Tris (pH 7.4), 150 mM NaCl, 0.5 mM EGTA, 0.5 mM EDTA, 0.5 mM DTT, 0.125 mM Na₃VO₄, 0.2 mM PMSF, 2 $\mu\text{g}/\text{mL}$ leupeptin, 2 $\mu\text{g}/\text{mL}$ aprotinin, 2 mM NaF, 0.25 mM Na₂P₂O₇, and 1% Triton X-100) prepared with nuclease-free water and RNase inhibitors (RNAsin 40 U/ μL , INVITROGEN, California, USA). The resulting homogenate was divided into separate aliquots for RNA extraction and protein levels determination.

Immunoblot Analysis. The whole hippocampus homogenate was sonicated on ice for 10 min and then centrifuged at 17,860g for 30 min. The supernatant was collected, and a sample was saved for protein determination using the bicinchoninic method (Pierce BCA Protein Assay Kit, Thermo Fisher Scientific). The remaining supernatant was boiled immediately in a sample loading buffer. A total of 25 to 50 μg of each protein extract was resolved on 12% SDS-polyacrylamide gels and then blotted onto 0.2 μm nitrocellulose or PVDF membranes. Membranes were finally processed for Western blot according to the conditions described in Table S1. After two 5 min rinses in Tris-buffered saline Tween 20, blots were incubated with peroxidase-conjugated secondary antibody at room temperature for 2 h. Membranes were developed by incubation with an enhanced chemiluminescent substrate (EZ-ECL, Biological Industries, Israel) and imaged with Syngene (Cambridge, UK). To detect protein bands with the same molecular weight (pCREB/CREB/ β -actin), we performed the stripping protocol using Ponceau red for 30 min, followed by extensive washes with PBS to ensure complete removal of previous antibodies before membrane reprobing. Bands were quantified with ImageJ (<https://imagej.nih.gov/ij>) and normalized to β -actin immunoreactivity as a loading control. In the case of pCREB, the results were expressed as a ratio of phosphorylated/total protein. Original immunoblots for each protein (Figure S1) are available in the Supporting Information.

miRNA Levels by Quantitative Real-Time PCR. miRNA isolation and quantitative real-time PCR was performed as described previously.^{10,27} Briefly, isolation of RNA < 200 nucleotides (nt) was performed with a RNeasy Mini Kit (Qiagen, Hilden, Germany), according to the manufacturer's protocol. RNA < 200 nt (100 ng) was then polyadenylated and simultaneously reverse transcribed with the miScript II RT kit (Qiagen, Hilden, Germany) including an oligo-dT tag primer and reverse transcriptase according to the manufacturer's instructions. qPCR experiments were conducted on an Mx3000p thermocycler (Stratagene/Agilent, La Jolla, CA) programmed as follows: 95 °C for 15 min, followed by 40 cycles of 94 °C for 15 s, 55 °C for 15 s, and 70 °C for 15 s. Primers were obtained from QIAGEN, and their sequences for

miR-16 (efficiency 85.8%), miR-134 (efficiency 90.1%), miR-138 (efficiency 83.4%), and miR-485 (efficiency 86.8%) were TAGCAGCACGTAATATTGGCG, TGTGACTGGTT-GACCAGAGGGG, AGCUGGUGUUGUGAAUCAGGCCG, and AGAGGCTGGCCGTGATGAATTG, respectively. The relative abundance of these miRNAs was relativized to the levels of small nucleolar RNA SNO95 with standard primers for amplification (efficiency 97.3%; catalog no. MS00033726; QIAGEN) and then normalized to control animals. Relative miRNA levels were calculated based on the $2^{-\Delta\Delta ct}$ normalized to that of the SNO gene RNA. All RT-PCRs and PCRs included the use of water in place of the template as a negative control and the input of RNA without the RT reaction.

Construction of PPI Networks. We constructed PPI networks for both sertraline and fasudil to establish whether these drugs share common targets that may explain their described common effects. The PPI network is depicted with nodes representing proteins and edges, indicating the interactions between them. To construct the PPIs, we retrieved all active targets for sertraline and fasudil from the ChEMBL database (v.31).⁷⁵ This retrieval relied on ChEMBL annotations and their pChEMBL values, which represent molecular potency as the negative log₁₀ of molar concentration for measurements such as IC₅₀, XC₅₀, EC₅₀, AC₅₀, K_i, K_d, and potency.⁷⁶ Target selection based on pChEMBL was guided by classification thresholds proposed by the National Institutes of Health (NIH) initiative Illuminating the Druggable Genome (IDG).⁷⁷ Then, with the identified targets, we independently extracted PPI for each target using the STRING database.⁷⁸ To ensure data robustness, interactions with experimental and/or database STRING scores ≥ 0.7 were kept using the Python NetworkX library.⁷⁹

To expand the PPIs, a second STRING search was conducted using the primary neighbors of the direct drug targets, thereby extending the network layer to the secondary neighbors (second PPI expansion, Figure 5). Finally, to effectively merge both expanded PPI networks, we combined all common interactions (edges) between them. Targets from both PPIs were maintained in the merging process. To maintain cohesive communities where nodes interact within the drugs-PPI network, we discarded unconnected components that did not significantly contribute to the overall structure. This approach ensured a more coherent and focused representation of the key interactions between fasudil and sertraline PPIs. In this study, we employed a methodological approach that involved three distinct analyses. Each analysis focused on merging the third drugs-PPI network with three different networks: the depression-related interaction network (D-PPI), the dendritic spine morphology protein network (DSM-PPI), and the network centered on miRNA hsa-miR-138-5p targets (miRNA-PPI). As a result of these mergers, three novel networks were created: drugs-D-PPI, drugs-DSM-PPI, and drugs-miRNA-PPI. Following each merger, we applied a specific tissue-based filtering process to each combined network. To obtain the following networks:

I Depression-Related Interaction Network (D-PPI): a PPI network was constructed by using the Open Targets database,⁸⁰ which involved proteins associated with Unipolar Depression (EFO_0003761), Major Depressive Disorder (MONDO_0002009), and Depressive Symptom Measurement (EFO_0007006) with scores of 0.5 or higher (score from the Open Targets database).

Additionally, the serotonin transporter (SLC6A4) and its interactors alpha-synuclein (SNCA) and syntaxin-1A (STX1A) were manually added as their interactions are key for the pharmacological effect² but did not meet the established thresholds. After combining this network with the drugs-PPI network, proteins expressed in the brain were filtered using information from the Human Protein Atlas, resulting in the final drugs-D-PPI.

II Dendritic Spine Morphology Protein Network (DSM-PPI): A PPI network based on proteins linked to changes in dendritic spine morphology⁸¹ was constructed. Following its merge with the drugs-PPI network, we obtained the drugs-DSM-PPI which only considers proteins expressed in the hippocampus, according to the Human Protein Atlas.

III Network Centered on miRNA hsa-miR-138-5p (miRNA-PPI): The third network focused on the miRNA hsa-miR138-5p was built using targets with strong evidence from the MiRTarBase database version 9.0.⁸² Once combined with the drugs-PPI network, a similar filtering was conducted to retain proteins expressed in the hippocampus as described above, resulting in the final drugs-miRNA-PPI.

Common Path Analysis. After constructing the three interaction networks (drugs-D-PPI, drugs-DSM-PPI, and drugs-miRNA-PPI), we conducted a comprehensive analysis for each one. This analysis aimed to identify all potential shared pathways between the drugs sertraline and fasudil, with a limit of four intermediaries. Starting from the targets of sertraline and fasudil as the initial points, the analysis proceeded toward the specific proteins of interest in each network as follows: (i) Drugs-D-PPI: end points were the targets related to depression. (ii) Drugs-DSM-PPI: end points were proteins linked to morphological changes in dendritic spines. (iii) Drugs-miRNA-PPI: end points were the targets related to hsa-miR-138-5p.

First, we used the “all_shortest_paths” algorithm from the Network X Python library to independently calculate all shortest paths from the targets of sertraline to their respective end points and from the targets of fasudil to their end points.

Next, we analyzed the paths based on their lengths. We considered direct paths (with no intermediaries) as well as paths that included one, two, three, or four intermediary nodes. For each path length, we identified common paths (paths that lead to the same end point). These paths can either be identical from the start to the end point or may diverge initially but converge at the first intermediary node, continuing along the same route to the end point.

Cross-Network Path Analysis. In addition to the initial analysis of the three final PPI networks, we implemented a second analysis that consisted of a comprehensive comparison of all PPIs. This analysis was conducted in two main stages:

I Global comparison: Initially, we identified the most important proteins by analyzing how often they appear in various paths within each network. We used a special scoring method, applying a formula where the score decreases logarithmically based on the number of intermediaries in the path. Specifically, the score is higher for proteins directly connected in the path and lower for those connected through more intermediaries. Therefore, the total score for each protein involved in any path was defined as follows

$$\text{total score} = \sum_{i=1}^4 10^{(5-i)} \cdot N_i$$

where N_i denotes the number of times a protein appears in a given path and i is the number of connections in these paths ranging from 1 (indicating a direct connection) to 5 (indicating four intermediaries). For example, the total score of one protein directly connected to another in a path is 10,000. In contrast, the total score of a protein that is only four steps away in the path (indicating it is connected through four other proteins) is 1. This scoring system helps us quantify the importance of each protein in the network. Next, we focused on proteins with a total score ≥ 2500 (cutoff), as this high score could indicate a significant role in the network's paths. To facilitate comparison across networks, these scores were then normalized using a min–max normalization approach, scaling the values to a range of 0 to 1. This step allowed us to pinpoint the most crucial proteins across the networks. We then compared these key proteins across the three different networks to find those that are common and significant in at least two networks.

II Local Comparison: In this analysis, we scrutinized the involvement of specific proteins within each network, particularly focusing on their roles in paths with no more than two intermediaries. For the drugs-D-PPI network, we investigated proteins linked to morphological changes and those targeted by miRNA hsa-miR-138-Sp. In the drugs-DSM-PPI network, we evaluated proteins associated with depression and targets of miRNA hsa-miR-138-Sp. Similarly, in the drugs-miRNA-PPI, we analyzed proteins connected to depression and morphological alterations.

These cross-network analyses revealed shared interactions and key interaction patterns, highlighting potentially vital proteins in mechanisms related to depression, dendritic morphology, and miRNA hsa-miR-138-Sp action.

Statistical Analysis. The statistical analyses were performed using statistical software GraphPad Prism 10.0.0 (GraphPad Software Inc., San Diego, CA, USA). The data are expressed as the mean \pm SEM (standard error of the mean) and were analyzed using two-way ANOVA, followed by Fisher's LSD test. Normality was assessed using the Shapiro-Wilk test before parametric statistical tests. All data sets successfully passed the normality test, confirming that the assumptions for parametric analysis were met. These analyses allowed for the determination of the effects of treatment (fasudil or sertraline) and stress and their interaction (treatment \times stress), as well as differences between groups. Table S2 shows detailed tests statistics.

■ ASSOCIATED CONTENT

SI Supporting Information

The Supporting Information is available free of charge at <https://pubs.acs.org/doi/10.1021/acsptsci.4c00680>.

PPI networks built in this study ([XLSX](#))

Original Western blot images, effect of stress and treatments on APT1 protein levels, path analysis subnetworks, path analysis of fasudil and sertraline targets, primary antibodies and Western blot conditions, and details of statistical tests ([PDF](#))

■ AUTHOR INFORMATION

Corresponding Authors

David Ramírez – Departamento de Farmacología, Facultad de Ciencias Biológicas, Universidad de Concepción, Concepción 4030000, Chile; [orcid.org/0000-0003-0002-1189](#); Email: dramirez@udec.cl

Jenny L. Fiedler – Laboratory of Neuroplasticity and Neurogenetics, Department of Biochemistry and Molecular Biology, Faculty of Chemical and Pharmaceutical Sciences, Universidad de Chile, Santiago 8380492, Chile; [orcid.org/0000-0002-3928-4325](#); Email: jfiedler@ciq.uchile.cl

Authors

Gonzalo García-Rojo – Laboratory of Neuroplasticity and Neurogenetics, Department of Biochemistry and Molecular Biology, Faculty of Chemical and Pharmaceutical Sciences, Universidad de Chile, Santiago 8380492, Chile; Departamento de Química, Facultad de Ciencias, Universidad de La Serena, La Serena 1700000, Chile; Present Address: Laboratorio de Señales Moleculares, Departamento de Química, Facultad de Ciencias, Universidad de La Serena, La Serena, Chile; [orcid.org/0000-0001-8135-6313](#)

Ignacio Valenzuela Martínez – Departamento de Farmacología, Facultad de Ciencias Biológicas, Universidad de Concepción, Concepción 4030000, Chile; Doctorado en Biotecnología Molecular, Facultad de Ciencias Biológicas, Universidad de Concepción, Concepción 4030000, Chile; [orcid.org/0000-0001-8538-8320](#)

Felipe Aguayo – Laboratory of Neuroplasticity and Neurogenetics, Department of Biochemistry and Molecular Biology, Faculty of Chemical and Pharmaceutical Sciences, Universidad de Chile, Santiago 8380492, Chile; Present Address: Signal Transduction Laboratory, National Institutes of Health, North Carolina, United States of America.; [orcid.org/0000-0002-9106-598X](#)

Mauricio Muñoz-Llanos – Laboratory of Neuroplasticity and Neurogenetics, Department of Biochemistry and Molecular Biology, Faculty of Chemical and Pharmaceutical Sciences, Universidad de Chile, Santiago 8380492, Chile; Present Address: Facultad de Medicina, Escuela de Química y Farmacia, Universidad Andres Bello, Concepción, Chile.; [orcid.org/0009-0009-8491-5091](#)

Complete contact information is available at:

<https://pubs.acs.org/10.1021/acsptsci.4c00680>

Author Contributions

^VG.G.-R. and I.V.M. share the first authorship. G.G., M.M., F.A., and J.L.F. designed the experiments. G.G. and F.A. performed the experiments and data analysis. D.R and I.V. performed the construction of Interaction Networks and Cross-Network common path analysis. The manuscript was written through contributions of all authors. All authors have given approval to the final version of the manuscript.

Funding

This study was supported by FONDECYT 11241164 (García-Rojo G.), FONDECYT 1230471 (JL Fiedler), FONDECYT 1220656 (Ramírez, D), and DIDULS PR23211213 (García-Rojo G.).

Notes

The authors declare no competing financial interest.

■ REFERENCES

- (1) Vos, T.; Lim, S. S.; Abbafati, C.; Abbas, K. M.; Abbasi, M.; Abbasifard, M.; Abbasi-Kangevari, M.; Abbastabar, H.; Abd-Allah, F.; Abdelalim, A.; Abdollahi, M.; Abdollahpour, I.; Abolhassani, H.; Aboyan, V.; Abrams, E. M.; Abreu, L. G.; Abrigo, M. R. M.; Abu-Raddad, L. J.; Abushouk, A. I.; Acebedo, A.; Ackerman, I. N.; Adabi, M.; Adamu, A. A.; Adebayo, O. M.; Adekanmbi, V.; Adelson, J. D.; Adetokunboh, O. O.; Adham, D.; Afshari, M.; Afshin, A.; Agardh, E. E.; Agarwal, G.; Agesa, K. M.; Aghaali, M.; Aghamir, S. M. K.; Agrawal, A.; Ahmad, T.; Ahmad, A.; Ahmadi, M.; Ahmadi, H.; Ahmadpour, E.; Akalu, T. Y.; Akinyemi, R. O.; Akinyemiju, T.; Akombi, B.; Al-Aly, Z.; Alam, K.; Alam, N.; Alam, S.; Alam, T.; Alanzi, T. M.; Albertson, S. B.; Alcalde-Rabanal, J. E.; Alema, N. M.; Ali, M.; Ali, S.; Alicandro, G.; Alizanazadeh, M.; Alinia, C.; Alipour, V.; Aljunid, S. M.; Alla, F.; Allebeck, P.; Almasi-Hashiani, A.; Alonso, J.; Al-Raddadi, R. M.; Altirkawi, K. A.; Alvis-Guzman, N.; Alvis-Zakzuk, N. J.; Amini, S.; Amini-Rarani, M.; Aminorroaya, A.; Amiri, F.; Amit, A. M. L.; Amugsi, D. A.; Amul, G. G. H.; Anderlini, D.; Andrei, C. L.; Andrei, T.; Anjomshoa, M.; Ansari, F.; Ansari, I.; Ansari-Moghaddam, A.; Antonio, C. A. T.; Antony, C. M.; Antriayandarti, E.; Anvari, D.; Anwer, R.; Arabloo, J.; Arab-Zozani, M.; Aravkin, A. Y.; Ariani, F.; Ärnlöv, J.; Aryal, K. K.; Arzani, A.; Asadi-Aliabadi, M.; Asadi-Pooya, A. A.; Asghari, B.; Ashbaugh, C.; Atnafu, D. D.; Atre, S. R.; Ausloos, F.; Ausloos, M.; Ayala Quintanilla, B. P.; Ayano, G.; Ayanore, M. A.; Aynalem, Y. A.; Azari, S.; Azarian, G.; Azene, Z. N.; Babaee, E.; Badawi, A.; Bagherzadeh, M.; Bakhshaei, M. H.; Bakhtiari, A.; Balakrishnan, S.; Balalla, S.; Balassano, S.; Banach, M.; Banik, P. C.; Bannick, M. S.; Bante, A. B.; Baraki, A. G.; Barboza, M. A.; Barker-Collo, S. L.; Barthélémy, C. M.; Barua, L.; Barzegar, A.; Basu, S.; Baune, B. T.; Bayati, M.; Bazmandegan, G.; Bedi, N.; Beghi, E.; Béjot, Y.; Bello, A. K.; Bender, R. G.; Bennett, D. A.; Bennett, F. B.; Bensenor, I. M.; Benziger, C. P.; Berhe, K.; Bernabe, E.; Bertolacci, G. J.; Bhageerathy, R.; Bhala, N.; Bhandari, D.; Bhardwaj, P.; Bhattacharyya, K.; Bhutta, Z. A.; Bibi, S.; Biehl, M. H.; Bikbov, B.; Bin Sayeed, M. S.; Biondi, A.; Birihane, B. M.; Bisanzio, D.; Bisignano, C.; Biswas, R. K.; Bohloul, S.; Bohluli, M.; Bolla, S. R. R.; Boloor, A.; Boon-Dooley, A. S.; Borges, G.; Borzì, A. M.; Bourne, R.; Brady, O. J.; Brauer, M.; Brayne, C.; Breitborde, N. J. K.; Brenner, H.; Briant, P. S.; Briggs, A. M.; Briko, N. I.; Britton, G. B.; Bryazka, D.; Buchbinder, R.; Bumgarner, B. R.; Busse, R.; Butt, Z. A.; Caetano dos Santos, F. L.; Cámera, L. L. A.; Campos-Nonato, I. R.; Car, J.; Cárdenas, R.; Carreras, G.; Carrero, J. J.; Carvalho, F.; Castaldelli-Maia, J. M.; Castañeda-Orjuela, C. A.; Castelpietra, G.; Castle, C. D.; Castro, F.; Catalá-López, F.; Causey, K.; Cederroth, C. R.; Cercy, K. M.; Cerin, E.; Chandan, J. S.; Chang, A. R.; Charlson, F. J.; Chattu, V. K.; Chaturvedi, S.; Chimed-Ochir, O.; Chin, K. L.; Cho, D. Y.; Christensen, H.; Chu, D.-T.; Chung, M. T.; Cicuttini, F. M.; Ciobanu, L. G.; Cirillo, M.; Collins, E. L.; Compton, K.; Conti, S.; Cortesi, P. A.; Costa, V. M.; Cousin, E.; Cowden, R. G.; Cowie, B. C.; Cromwell, E. A.; Cross, D. H.; Crowe, C. S.; Cruz, J. A.; Cunningham, M.; Dahlawi, S. M. A.; Damiani, G.; Dandona, L.; Dandona, R.; Darwesh, A. M.; Daryani, A.; Das, J. K.; Das Gupta, R.; das Neves, J.; Dávila-Cervantes, C. A.; Davletov, K.; De Leo, D.; Dean, F. E.; DeCleene, N. K.; Deen, A.; Degenhardt, L.; Dellavalle, R. P.; Demeke, F. M.; Demsie, D. G.; Denova-Gutiérrez, E.; Dereje, N. D.; Dervenis, N.; Desai, R.; Desalew, A.; Dessie, G. A.; Dharmaratne, S. D.; Dhungana, G. P.; Dianatinasab, M.; Diaz, D.; Dibaji Forooshani, Z. S.; Dingels, Z. V.; Dirac, M. A.; Djalalinia, S.; Do, H. T.; Dokova, K.; Dorostkar, F.; Doshi, C. P.; Doshmangir, L.; Douiri, A.; Doxey, M. C.; Driscoll, T. R.; Dunachie, S. J.; Duncan, B. B.; Duraes, A. R.; Eagan, A. W.; Ebrahimi Kalan, M.; Edvardsson, D.; Ehrlich, J. R.; El Nahas, N.; El Sayed, I.; El Tantawi, M.; Elbarazi, I.; Elgendi, I. Y.; Elhabashy, H. R.; El-Jaafary, S. I.; Elyazar, I. R.; Emamian, M. H.; Emmons-Bell, S.; Erskine, H. E.; Eshrat, B.; Eskandarieh, S.; Esmaeilnejad, S.; Esmaeilzadeh, F.; Esteghamati, A.; Estep, K.; Etemadi, A.; Etisso, A. E.; Farahmand, M.; Faraj, A.; Fareed, M.; Faridnia, R.; Farinha, C. S. e; Farioli, A.; Faro, A.; Faruque, M.; Farzadfar, F.; Fattahi, N.; Fazlzadeh, M.; Feigin, V. L.; Feldman, R.; Fereshtehnejad, S.-M.; Fernandes, E.; Ferrari, A. J.; Ferreira, M. L.; Filip, I.; Fischer, F.; Fisher, J. L.; Fitzgerald, R.; Flohr, C.; Flor, L. S.; Foigt, N. A.; Folayan, M. O.; Force, L. M.; Fornari, C.; Foroutan, M.; Fox, J. T.; Freitas, M.; Fu, W.; Fukumoto, T.; Furtado, J. M.; Gad, M. M.; Gakidou, E.; Galles, N. C.; Gallus, S.; Gamkrelidze, A.; Garcia-Basteiro, A. L.; Gardner, W. M.; Geberemariyam, B. S.; Gebrehiwot, A. M.; Gebremedhin, K. B.; Gebreslassie, A. A. A. A.; Gershberg Hayoon, A.; Gething, P. W.; Ghadimi, M.; Ghadiri, K.; Ghafourifard, M.; Ghajar, A.; Ghamari, F.; Ghashghaee, A.; Ghiasvand, H.; Ghith, N.; Gholamian, A.; Gilani, S. A.; Gill, P. S.; Gitimoghaddam, M.; Giussani, G.; Goli, S.; Gomez, R. S.; Gopalani, S. V.; Gorini, G.; Gorman, T. M.; Gottlich, H. C.; Goudarzi, H.; Goulart, A. C.; Goulart, B. N. G.; Grada, A.; Grivna, M.; Grossi, G.; Gubari, M. I. M.; Gugnani, H. C.; Guimaraes, A. L. S.; Guimaraes, R. A.; Guled, R. A.; Guo, G.; Guo, Y.; Gupta, R.; Haagsma, J. A.; Haddock, B.; Hafezi-Nejad, N.; Hafiz, A.; Hagins, H.; Haile, L. M.; Hall, B. J.; Halvaei, I.; Hamadeh, R. R.; Hamagharib Abdullah, K.; Hamilton, E. B.; Han, C.; Han, H.; Hankey, G. J.; Haro, J. M.; Harvey, J. D.; Hasaballah, A. I.; Hasanzadeh, A.; Hashemian, M.; Hassaniipour, S.; Hassankhani, H.; Havmoeller, R. J.; Hay, R. J.; Hay, S. I.; Hayat, K.; Heidari, B.; Heidari, G.; Heidari-Soureshjani, R.; Hendrie, D.; Henrikson, H. J.; Henry, N. J.; Hertelius, C.; Heydarpour, F.; Hird, T. R.; Hoek, H. W.; Hole, M. K.; Holla, R.; Hoogar, P.; Hosgood, H. D.; Hosseinzadeh, M.; Hostiuc, M.; Hostiuc, S.; Househ, M.; Hoy, D. G.; Hsairi, M.; Hsieh, V. C.; Hu, G.; Huda, T. M.; Hugo, F. N.; Huynh, C. K.; Hwang, B.-F.; Iannucci, V. C.; Ibitoye, S. E.; Ikuta, K. S.; Ilesanmi, O. S.; Ilic, I. M.; Ilic, M. D.; Inbaraj, L. R.; Ippolito, H.; Irvani, S. S. N.; Islam, M. M.; Islam, M.; Islam, S. M. S.; Islami, F.; Iso, H.; Ivers, R. Q.; Iwu, C. C. D.; Iyamu, I. O.; Jaafari, J.; Jacobsen, K. H.; Jadidi-Niaragh, F.; Jafari, H.; Jafarinia, M.; Jahagirdar, D.; Jahani, M. A.; Jahanmehr, N.; Jakovljevic, M.; Jalali, A.; Jalilian, F.; James, S. L.; Janjani, H.; Janodia, M. D.; Jayatilleke, A. U.; Jeemon, P.; Jenabi, E.; Jha, R. P.; Jha, V.; Ji, J. S.; Jia, P.; John, O.; John-Akinola, Y. O.; Johnson, C. O.; Johnson, S. C.; Jonas, J. B.; Joo, T.; Joshi, A.; Jozwiak, J. J.; Jürisson, M.; Kabir, A.; Kabir, Z.; Kalani, H.; Kalani, R.; Kalankesh, L. R.; Kalhor, R.; Kamiab, Z.; Kanchan, T.; Karami Matin, B.; Karch, A.; Karim, M. A.; Karimi, S. E.; Kassa, G. M.; Kassebaum, N. J.; Katikireddi, S. V.; Kawakami, N.; Kayode, G. A.; Keddie, S. H.; Keller, C.; Kereselidze, M.; Khafaie, M. A.; Khalid, N.; Khan, M.; Khatab, K.; Khater, M. M.; Khatib, M. N.; Khayamzadeh, M.; Khodayari, M. T.; Khundkar, R.; Kianipour, N.; Kieling, C.; Kim, D.; Kim, Y.-E.; Kim, Y. J.; Kimokoti, R. W.; Kisa, A.; Kisa, S.; Kissimova-Skarbek, K.; Kivimäki, M.; Kneib, C. J.; Knudsen, A. K. S.; Kocarnik, J. M.; Kolola, T.; Kopec, J. A.; Kosen, S.; Koul, P. A.; Koyanagi, A.; Kravchenko, M. A.; Krishan, K.; Krohn, K. J.; Kuade Defo, B.; Kucuk Bicer, B.; Kumar, G. A.; Kumar, M.; Kumar, P.; Kumar, V.; Kumaresh, G.; Kurmi, O. P.; Kusuma, D.; Kyu, H. H.; La Vecchia, C.; Lacey, B.; Lal, D. K.; Laloo, R.; Lam, J. O.; Lami, F. H.; Landires, I.; Lang, J. J.; Lansingh, V. C.; Larson, S. L.; Larsson, A. O.; Lasrado, S.; Lassi, Z. S.; Lau, K. M.-M.; Lavados, P. M.; Lazarus, J. V.; Ledesma, J. R.; Lee, P. H.; Lee, S. W. H.; LeGrand, K. E.; Leigh, J.; Leonardi, M.; Lescinsky, H.; Leung, J.; Levi, M.; Lewington, S.; Li, S.; Lim, L.-L.; Lin, C.; Lin, R.-T.; Linehan, C.; Linn, S.; Liu, H.-C.; Liu, S.; Liu, Z.; Looker, K. J.; Lopez, A. D.; Lopukhov, P. D.; Lorkowski, S.; Lotufo, P. A.; Lucas, T. C. D.; Lugo, A.; Lunevicius, R.; Lyons, R. A.; Ma, J.; MacLachlan, J. H.; Maddison, E. R.; Maddison, R.; Madotto, F.; Mahasha, P. W.; Mai, H. T.; Majeed, A.; Maled, V.; Maleki, S.; Malekzadeh, R.; Malta, D. C.; Mamun, A. A.; Manafi, A.; Manafi, N.; Manguerra, H.; Mansouri, B.; Mansournia, M. A.; Mantilla Herrera, A. M.; Maravilla, J. C.; Marks, A.; Martins-Melo, F. R.; Martopullo, I.; Masoumi, S. Z.; Massano, J.; Massenburg, B. B.; Mathur, M. R.; Maulik, P. K.; McAlinden, C.; McGrath, J. J.; McKee, M.; Mehndiratta, M. M.; Mehri, F.; Mehta, K. M.; Meitei, W. B.; Memiah, P. T. N.; Mendoza, W.; Menezes, R. G.; Mengesha, E. W.; Mengesha, M. B.; Mereke, A.; Meretoja, A.; Meretoja, T. J.; Mestrovic, T.; Miazgowski, B.; Miazgowski, T.; Michalek, I. M.; Mihretie, K. M.; Miller, T. R.; Mills, E. J.; Mirica, A.; Mirrakhimov, E. M.; Mirzaei, H.; Mirzaei, M.;

Mirzaei-Alavijeh, M.; Misganaw, A. T.; Mithra, P.; Moazen, B.; Moghadaszadeh, M.; Mohamadi, E.; Mohammad, D. K.; Mohammad, Y.; Mohammad Gholi Mezerji, N.; Mohammadian-Hafshejani, A.; Mohammadifard, N.; Mohammadpourhodki, R.; Mohammed, S.; Mokdad, A. H.; Molokhia, M.; Momen, N. C.; Monasta, L.; Mondello, S.; Mooney, M. D.; Moosazadeh, M.; Moradi, G.; Moradi, M.; Moradi-Lakeh, M.; Moradzadeh, R.; Moraga, P.; Morales, L.; Morawska, L.; Moreno Velásquez, I.; Morgado-da-Costa, J.; Morrison, S. D.; Mosser, J. F.; Mouodi, S.; Mousavi, S. M.; Mousavi Khanegah, A.; Mueller, U. O.; Munro, S. B.; Muriithi, M. K.; Musa, K. I.; Muthupandian, S.; Naderi, M.; Nagarajan, A. J.; Nagel, G.; Naghshtabrizi, B.; Nair, S.; Nandi, A. K.; Nangia, V.; Nansseu, J. R.; Nayak, V. C.; Nazari, J.; Negoi, I.; Negoi, R. I.; Netsere, H. B. N.; Ngunjiri, J. W.; Nguyen, C. T.; Nguyen, J.; Nguyen, M.; Nguyen, M.; Nichols, E.; Nigatu, D.; Nigatu, Y. T.; Nikbaksh, R.; Nixon, M. R.; Nnaji, C. A.; Nomura, S.; Norrving, B.; Noubiap, J. J.; Nowak, C.; Nunez-Samudio, V.; Otoju, A.; Oancea, B.; Odell, C. M.; Ogbo, F. A.; Oh, I.-H.; Okunga, E. W.; Oladnabi, M.; Olagunju, A. T.; Olusanya, B. O.; Olusanya, J. O.; Oluwasanu, M. M.; Omar Bali, A.; Omer, M. O.; Ong, K. L.; Onwujekwe, O. E.; Orji, A. U.; Orpana, H. M.; Ortiz, A.; Ostroff, S. M.; Oststavnov, N.; Oststavnov, S. S.; Øverland, S.; Owolabi, M. O.; P A, M.; Padubidri, J. R.; Pakhare, A. P.; Palladino, R.; Pana, A.; Panda-Jonas, S.; Pandey, A.; Park, E.-K.; Parmar, P. G. K.; Pasupula, D. K.; Patel, S. K.; Paternina-Caicedo, A. J.; Pathak, A.; Pathak, M.; Patten, S. B.; Patton, G. C.; Paudel, D.; Pazoki Toroudi, H.; Peden, A. E.; Pennini, A.; Pepito, V. C. F.; Peprah, E. K.; Pereira, A.; Pereira, D. M.; Perico, N.; Pham, H. Q.; Phillips, M. R.; Pigott, D. M.; Pilgrim, T.; Pilz, T. M.; Pirsahib, M.; Plana-Ripoll, O.; Plass, D.; Pokhrel, K. N.; Polibin, R. V.; Polinder, S.; Polkinghorne, K. R.; Postma, M. J.; Pourjafar, H.; Pourmalek, F.; Pourmirza Kalhor, R.; Pourshams, A.; Poznańska, A.; Prada, S. I.; Prakash, V.; Pribadi, D. R. A.; Pupillo, E.; Quazi Syed, Z.; Rabiee, M.; Rabiee, N.; Radfar, A.; Rafiee, A.; Rafiee, A.; Raggi, A.; Rahimi-Movaghhar, A.; Rahman, M. A.; Rajabpour-Sanati, A.; Rajati, F.; Ramezanadeh, K.; Ranabhat, C. L.; Rao, P. C.; Rao, S. J.; Rasella, D.; Rastogi, P.; Rathi, P.; Rawaf, D. L.; Rawaf, S.; Rawal, L.; Razo, C.; Redford, S. B.; Reiner, R. C.; Reinig, N.; Reitsma, M. B.; Remuzzi, G.; Renjith, V.; Renzaho, A. M. N.; Resnikoff, S.; Rezaei, N.; Rezai, M. S.; Rezapour, A.; Rhinehart, P.-A.; Riahi, S. M.; Ribeiro, A. L. P.; Ribeiro, D. C.; Ribeiro, D.; Rickard, J.; Roberts, N. L. S.; Roberts, S.; Robinson, S. R.; Roever, L.; Rolfe, S.; Ronfani, L.; Rosenthal, G.; Roth, G. A.; Rubagotti, E.; Rumisha, S. F.; Sabour, S.; Sachdev, P. S.; Saddik, B.; Sadeghi, E.; Sadeghi, M.; Saeidi, S.; Safi, S.; Safiri, S.; Sagar, R.; Sahebkar, A.; Sahraian, M. A.; Sajadi, S. M.; Salahshoor, M. R.; Salamat, P.; Salehi Zahabi, S.; Salem, H.; Salem, M. R. R.; Salimzadeh, H.; Salomon, J. A.; Salz, I.; Samad, Z.; Samy, A. M.; Sanabria, J.; Santomauro, D. F.; Santos, I. S.; Santos, J. V.; Santric-Milicevic, M. M.; Saraswathy, S. Y. I.; Sarmiento-Suárez, R.; Sarrafzadegan, N.; Sartorius, B.; Sarveazad, A.; Sathian, B.; Sathish, T.; Sattin, D.; Sbarra, A. N.; Schaeffer, L. E.; Schiavolin, S.; Schmidt, M. I.; Schutte, A. E.; Schwebel, D. C.; Schwendicke, F.; Senbeta, A. M.; Senthilkumaran, S.; Sepanlou, S. G.; Shackelford, K. A.; Shadid, J.; Shahabi, S.; Shaheen, A. A.; Shaikh, M. A.; Shalash, A. S.; Shams-Beyranvand, M.; Shamsizadeh, M.; Shannawaz, M.; Sharafi, K.; Sharara, F.; Sheena, B. S.; Sheikhtaheri, A.; Shetty, R. S.; Shibuya, K.; Shiferaw, W. S.; Shigematsu, M.; Shin, J. I.; Shiri, R.; Shirkoohi, R.; Shrime, M. G.; Shuval, K.; Siabani, S.; Sigfusdottir, I. D.; Sigurvinssdottir, R.; Silva, J. P.; Simpson, K. E.; Singh, A.; Singh, J. A.; Skiadaresi, E.; Skou, S. T.; Skryabin, V. Y.; Sobngwi, E.; Sokhan, A.; Soltani, S.; Sorensen, R. J. D.; Soriano, J. B.; Sorrie, M. B.; Soyiri, I. N.; Seeramareddy, C. T.; Stanaway, J. D.; Stark, B. A.; Stefan, S. C.; Stein, C.; Steiner, C.; Steiner, T. J.; Stokes, M. A.; Stovner, L. J.; Stubbs, J. L.; Sudaryanto, A.; Sufiyan, M. B.; Sulo, G.; Sultan, I.; Sykes, B. L.; Sylte, D. O.; Szócska, M.; Tabarés-Seisdedos, R.; Tabb, K. M.; Tadakambla, S. K.; Taherkhani, A.; Tajdini, M.; Takahashi, K.; Taveira, N.; Teagle, W. L.; Teamé, H.; Tehrani-Baniashechi, A.; Teklehaymanot, B. F.; Terrason, S.; Tessema, Z. T.; Thankappan, K. R.; Thomson, A. M.; Tohidinik, H. R.; Tonelli, M.; Topor-Madry, R.; Torre, A. E.; Touvier, M.; Tovani-Palone, M. R. R.; Tran, B. X.

Travillian, R.; Troeger, C. E.; Truelson, T. C.; Tsai, A. C.; Tsatsakis, A.; Tudor Car, L.; Tyrovolas, S.; Uddin, R.; Ullah, S.; Undurraga, E. A.; Unnikrishnan, B.; Vacante, M.; Vakilian, A.; Valdez, P. R.; Varughese, S.; Vasankari, T. J.; Vasseghian, Y.; Venketasubramanian, N.; Violante, F. S.; Vlassov, V.; Vollset, S. E.; Vongpradith, A.; Vukovic, A.; Vukovic, R.; Waheed, Y.; Walters, M. K.; Wang, J.; Wang, Y.; Wang, Y.-P.; Ward, J. L.; Watson, A.; Wei, J.; Weintraub, R. G.; Weiss, D. J.; Weiss, J.; Westerman, R.; Whisman, J. L.; Whiteford, H. A.; Wiangkham, T.; Wiens, K. E.; Wijeratne, T.; Wilner, L. B.; Wilson, S.; Wojtyniak, B.; Wolfe, C. D. A.; Wool, E. E.; Wu, A.-M.; Wulf Hanson, S.; Wunrow, H. Y.; Xu, G.; Xu, R.; Yadgir, S.; Yahyazadeh Jabbari, S. H.; Yamagishi, K.; Yaminfirooz, M.; Yano, Y.; Yaya, S.; Yazdi-Feyzabadi, V.; Yearwood, J. A.; Yeheyis, T. Y.; Yeshitila, Y. G.; Yip, P.; Yonemoto, N.; Yoon, S.-J.; Yousefi Lebni, J.; Younis, M. Z.; Younker, T. P.; Yousefi, Z.; Yousefifard, M.; Yousefinezhadi, T.; Yousuf, A. Y.; Yu, C.; Yusefzadeh, H.; Zahrian Moghadam, T.; Zaki, L.; Zaman, S. B.; Zamani, M.; Zamanian, M.; Zandian, H.; Zangeneh, A.; Zastrozhin, M. S.; Zewdie, K. A.; Zhang, Y.; Zhang, Z.-J.; Zhao, J. T.; Zhao, Y.; Zheng, P.; Zhou, M.; Ziapour, A.; Zimsen, S. R. M.; Naghavi, M.; Murray, C. J. L.; GBD 2019 Diseases and Injuries Collaborators. Global Burden of 369 Diseases and Injuries in 204 Countries and Territories, 1990–2019: A Systematic Analysis for the Global Burden of Disease Study 2019. *Lancet* **2020**, *396* (10258), 1204–1222.

(2) Bogowicz, P.; Curtis, H. J.; Walker, A. J.; Cowen, P.; Geddes, J.; Goldacre, B. Trends and Variation in Antidepressant Prescribing in English Primary Care: A Retrospective Longitudinal Study. *BJGP Open* **2021**, *5* (4), BJGPO.2021.0020.

(3) Gelenberg, A.; Chesen, C. How Fast Are Antidepressants? *J. Clin. Psychiatry* **2000**, *61* (10), 712–721.

(4) Racagni, G.; Popoli, M. Cellular and Molecular Mechanisms in the Long-Term Action of Antidepressants. *Dialogues Clin. Neurosci.* **2008**, *10* (4), 385–400.

(5) Sullivan, P. F.; Neale, M. C.; Kendler, K. S. Genetic Epidemiology of Major Depression: Review and Meta-Analysis. *Am. J. Psychiatry* **2000**, *157*, 1552–1562.

(6) LeMoult, J. From Stress to Depression: Bringing Together Cognitive and Biological Science. *Curr. Dir. Psychol. Sci.* **2020**, *29* (6), 592–598.

(7) Santomauro, D. F.; Mantilla Herrera, A. M.; Shadid, J.; Zheng, P.; Ashbaugh, C.; Pigott, D. M.; Abbafati, C.; Adolph, C.; Amlag, J. O.; Aravkin, A. Y.; Bang-Jensen, B. L.; Bertolacci, G. J.; Bloom, S. S.; Castellano, R.; Castro, E.; Chakrabarti, S.; Chattopadhyay, J.; Cogen, R. M.; Collins, J. K.; Dai, X.; Dangel, W. J.; Dapper, C.; Deen, A.; Erickson, M.; Ewald, S. B.; Flaxman, A. D.; Frostad, J. J.; Fullman, N.; Giles, J. R.; Giref, A. Z.; Guo, G.; He, J.; Helak, M.; Hulland, E. N.; Idrisov, B.; Lindstrom, A.; Linebarger, E.; Lotufo, P. A.; Lozano, R.; Magistro, B.; Malta, D. C.; Måansson, J. C.; Marinho, F.; Mokdad, A. H.; Monasta, L.; Naik, P.; Nomura, S.; O'Halloran, J. K.; Ostroff, S. M.; Pasovic, M.; Penberthy, L.; Reiner, R. C.; Reinke, G.; Ribeiro, A. L. P.; Sholokhov, A.; Sorensen, R. J. D.; Varavikova, E.; Vo, A. T.; Walcott, R.; Watson, S.; Wiysonge, C. S.; Zigler, B.; Hay, S. I.; Vos, T.; Murray, C. J. L.; Whiteford, H. A.; Ferrari, A. J. Global Prevalence and Burden of Depressive and Anxiety Disorders in 204 Countries and Territories in 2020 Due to the COVID-19 Pandemic. *Lancet* **2021**, *398* (10312), 1700–1712.

(8) Bravo, J. A.; Díaz-Veliz, G.; Mora, S.; Ulloa, J. L.; Berthoud, V. M.; Morales, P.; Arancibia, S.; Fiedler, J. L. Desipramine Prevents Stress-Induced Changes in Depressive-like Behavior and Hippocampal Markers of Neuroprotection. *Behav. Pharmacol.* **2009**, *20* (3), 273–285.

(9) Ulloa, J. L.; Castañeda, P.; Berrios, C.; Díaz-Veliz, G.; Mora, S.; Bravo, J. A.; Araneda, K.; Menares, C.; Morales, P.; Fiedler, J. L. Comparison of the Antidepressant Sertraline on Differential Depression-like Behaviors Elicited by Restraint Stress and Repeated Corticosterone Administration. *Pharmacol., Biochem. Behav.* **2010**, *97* (2), 213–221.

(10) Castañeda, P.; Muñoz, M.; García-Rojo, G.; Ulloa, J. L.; Bravo, J. A.; Márquez, R.; García-Pérez, M. A.; Arancibia, D.; Araneda, K.;

- Rojas, P. S.; Mondaca-Ruff, D.; Díaz-Véliz, G.; Mora, S.; Aliaga, E.; Fiedler, J. L. Association of N-Cadherin Levels and Downstream Effectors of Rho GTPases with Dendritic Spine Loss Induced by Chronic Stress in Rat Hippocampal Neurons. *J. Neurosci. Res.* **2015**, *93* (10), 1476.
- (11) Nestler, E. J.; Hyman, S. E. Animal Models of Neuropsychiatric Disorders. *Nat. Neurosci.* **2010**, *13*, 1161–1169.
- (12) Lee, T.; Jarome, T.; Li, S. J.; Kim, J. J.; Helmstetter, F. J. Chronic Stress Selectively Reduces Hippocampal Volume in Rats: A Longitudinal Magnetic Resonance Imaging Study. *Neuroreport* **2009**, *20* (17), 1554–1558.
- (13) MacQueen, G. M.; Campbell, S.; McEwen, B. S.; Macdonald, K.; Amano, S.; Joffe, R. T.; Nahmias, C.; Young, L. T.; Milliken Hatch, M. Course of Illness, Hippocampal Function, and Hippocampal Volume in Major Depression. *Proc. Natl. Acad. Sci. U.S.A.* **2003**, *100*, 1387–1392.
- (14) Qiao, H.; Li, M. X.; Xu, C.; Chen, H. B.; An, S. C.; Ma, X. M. Dendritic Spines in Depression: What We Learned from Animal Models. *Neural Plast.* **2016**, *2016*, 1–26.
- (15) Banasr, M.; Dwyer, J. M.; Duman, R. S. Cell Atrophy and Loss in Depression: Reversal by Antidepressant Treatment. *Curr. Opin. Cell Biol.* **2011**, *23*, 730–737.
- (16) Duman, R. S.; Voleti, B. Signaling Pathways Underlying the Pathophysiology and Treatment of Depression: Novel Mechanisms for Rapid-Acting Agents. *Trends Neurosci.* **2012**, *35*, 47–56.
- (17) Guan, L.; Jia, N.; Zhao, X.; Zhang, X.; Tang, G.; Yang, L.; Sun, H.; Wang, D.; Su, Q.; Song, Q.; Cai, D.; Cai, Q.; Li, H.; Zhu, Z. The Involvement of ERK/CREB/Bcl-2 in Depression-like Behavior in Prenatally Stressed Offspring Rats. *Brain Res. Bull.* **2013**, *99*, 1–8.
- (18) Qi, X.; Lin, W.; Li, J.; Li, H.; Wang, W.; Wang, D.; Sun, M. Fluoxetine Increases the Activity of the ERK-CREB Signal System and Alleviates the Depressive-like Behavior in Rats Exposed to Chronic Forced Swim Stress. *Neurobiol. Dis.* **2008**, *31* (2), 278–285.
- (19) Wang, J. Q.; Mao, L. The ERK Pathway: Molecular Mechanisms and Treatment of Depression. *Mol. Neurobiol.* **2019**, *56*, 6197–6205.
- (20) Manoharan, A.; Paul, A. Emerging Role of MicroRNAs as Novel Targets of Antidepressants. *Asian J. Psychiatry* **2021**, *66*, 102906.
- (21) Kosik, K. S. The Neuronal MicroRNA System. *Nat. Rev. Neurosci.* **2006**, *7*, 911–920.
- (22) Román-Albasini, L.; Díaz-Véliz, G.; Olave, F. A.; Aguayo, F. I.; García-Rojo, G.; Corrales, W. A.; Silva, J. P.; Ávalos, A. M.; Rojas, P. S.; Aliaga, E.; Fiedler, J. L. Antidepressant-Relevant Behavioral and Synaptic Molecular Effects of Long-Term Fasudil Treatment in Chronically Stressed Male Rats. *Neurobiol. Stress* **2020**, *13*, 100234.
- (23) García-Rojo, G.; Fresno, C.; Vilches, N.; Díaz-Véliz, G.; Mora, S.; Aguayo, F.; Pacheco, A.; Parra-Fiedler, N.; Parra, C. S.; Rojas, P. S.; Tejos, M.; Aliaga, E.; Fiedler, J. L. The ROCK Inhibitor Fasudil Prevents Chronic Restraint Stress-Induced Depressive-like Behaviors and Dendritic Spine Loss in Rat Hippocampus. *Int. J. Neuropsychopharmacol.* **2017**, *20* (4), 336.
- (24) Shapiro, L. P.; Kietzman, H. W.; Guo, J.; Rainnie, D. G.; Gourley, S. L. Rho-Kinase Inhibition Has Antidepressant-like Efficacy and Expedites Dendritic Spine Pruning in Adolescent Mice. *Neurobiol. Dis.* **2019**, *124*, 520–530.
- (25) Nakatake, Y.; Furuike, H.; Yamada, M.; Kuniishi, H.; Ukezono, M.; Yoshizawa, K.; Yamada, M. The Effects of Emotional Stress Are Not Identical to Those of Physical Stress in Mouse Model of Social Defeat Stress. *Neurosci. Res.* **2020**, *158*, 56–63.
- (26) Lai, K. O.; Ip, N. Y. Structural Plasticity of Dendritic Spines: The Underlying Mechanisms and Its Dysregulation in Brain Disorders. *Biochim. Biophys. Acta, Mol. Basis Dis.* **2013**, *1832*, 2257–2263.
- (27) Muñoz-Llanos, M.; García-Pérez, M. A.; Xu, X.; Tejos-Bravo, M.; Vidal, E. A.; Moyano, T. C.; Gutiérrez, R. A.; Aguayo, F. I.; Pacheco, A.; García-Rojo, G.; Aliaga, E.; Rojas, P. S.; Cidlowski, J. A.; Fiedler, J. L. MicroRNA Profiling and Bioinformatics Target Analysis in Dorsal Hippocampus of Chronically Stressed Rats: Relevance to Depression Pathophysiology. *Front. Mol. Neurosci.* **2018**, *11*, 251.
- (28) Fabbri, C.; Kasper, S.; Zohar, J.; Souery, D.; Montgomery, S.; Albani, D.; Forloni, G.; Ferentinos, P.; Rujescu, D.; Mendlewicz, J.; De Ronchi, D.; Riva, M. A.; Lewis, C. M.; Serretti, A. Drug Repositioning for Treatment-Resistant Depression: Hypotheses from a Pharmacogenomic Study. *Prog. Neuropsychopharmacol. Biol. Psychiatry* **2021**, *104*, 110050.
- (29) Jeong, J. Y.; Lee, D. H.; Kang, S. S. Effects of Chronic Restraint Stress on Body Weight, Food Intake, and Hypothalamic Gene Expressions in Mice. *Endocrinol. Metab.* **2013**, *28* (4), 288.
- (30) Zhang, Y.; Raap, D. K.; Garcia, F.; Serres, F.; Ma, Q.; Battaglia, G.; Van De Kar, L. D. Long-Term Fluoxetine Produces Behavioral Anxiolytic Effects without Inhibiting Neuroendocrine Responses to Conditioned Stress in Rats. *Brain Res.* **2000**, *855*, 58–66.
- (31) Nibuya, M.; Nestler, E. J.; Duman, R. S. Chronic Antidepressant Administration Increases the Expression of CAMP Response Element Binding Protein (CREB) in Rat Hippocampus. *J. Neurosci.* **1996**, *16*, 2365.
- (32) Errico, M.; Crozier, R. A.; Plummer, M. R.; Cowen, D. S. 5-HT₇ RECEPTORS ACTIVATE THE MITOGEN ACTIVATED PROTEIN KINASE EXTRACELLULAR SIGNAL RELATED KINASE IN CULTURED RAT HIPPOCAMPAL NEURONS. *Neuroscience* **2001**, *102*, 361–367.
- (33) Rojas, P. S.; Aguayo, F.; Neira, D.; Tejos, M.; Aliaga, E.; Muñoz, J. P.; Parra, C. S.; Fiedler, J. L. Dual Effect of Serotonin on the Dendritic Growth of Cultured Hippocampal Neurons: Involvement of 5-HT_{1A} and 5-HT₇ Receptors. *Mol. Cell. Neurosci.* **2017**, *85*, 148–161.
- (34) Blendy, J. A. The Role of CREB in Depression and Antidepressant Treatment. *Biol. Psychiatry* **2006**, *59*, 1144–1150.
- (35) Launay, J. M.; Mouillet-Richard, S.; Baudry, A.; Pietri, M.; Kellermann, O. Raphe-Mediated Signals Control the Hippocampal Response to SRI Antidepressants via MiR-16. *Transl. Psychiatry* **2011**, *1*, No. e56.
- (36) Murray, F.; Hutson, P. H. Hippocampal Bcl-2 Expression Is Selectively Increased Following Chronic but Not Acute Treatment with Antidepressants, 5-HT_{1A} or 5-HT_{2C/2B} Receptor Antagonists. *Eur. J. Pharmacol.* **2007**, *569* (1–2), 41–47.
- (37) Norrholm, S. D.; Ouimet, C. C. Altered Dendritic Spine Density in Animal Models of Depression and in Response to Antidepressant Treatment. *Synapse* **2001**, *42* (3), 151–163.
- (38) Chen, F.; Du Jardin, K. G.; Waller, J. A.; Sanchez, C.; Nyengaard, J. R.; Wegener, G. Vortioxetine Promotes Early Changes in Dendrite Morphology Compared to Fluoxetine in Rat Hippocampus. *Eur. Neuropsychopharmacol.* **2016**, *26* (2), 234–245.
- (39) Hajszan, T.; Dow, A.; Warner-Schmidt, J. L.; Szigeti-Buck, K.; Sallam, N. L.; Parducz, A.; Leranth, C.; Duman, R. S. Remodeling of Hippocampal Spine Synapses in the Rat Learned Helplessness Model of Depression. *Biol. Psychiatry* **2009**, *65* (5), 392–400.
- (40) Leuner, B.; Falduto, J.; Shors, T. J. Associative Memory Formation Increases the Observation of Dendritic Spines in the Hippocampus. *J. Neurosci.* **2003**, *23*, 659–665.
- (41) Chen, F.; Madsen, T. M.; Wegener, G.; Nyengaard, J. R. Imipramine Treatment Increases the Number of Hippocampal Synapses and Neurons in a Genetic Animal Model of Depression. *Hippocampus* **2010**, *20* (12), 1376–1384.
- (42) Wang, G.; Cheng, Y.; Gong, M.; Liang, B.; Zhang, M.; Chen, Y.; Zhang, C.; Yuan, X.; Xu, J. Systematic Correlation between Spine Plasticity and the Anxiety/Depression-like Phenotype Induced by Corticosterone in Mice. *Neuroreport* **2013**, *24* (12), 682–687.
- (43) Chen, F.; Madsen, T. M.; Wegener, G.; Nyengaard, J. R. Repeated Electroconvulsive Seizures Increase the Total Number of Synapses in Adult Male Rat Hippocampus. *Eur. Neuropsychopharmacol.* **2009**, *19* (5), 329–338.
- (44) Yang, C.; Shirayama, Y.; Zhang, J. C.; Ren, Q.; Yao, W.; Ma, M.; Dong, C.; Hashimoto, K.; R-Ketamine, K. R-ketamine: a rapid-onset and sustained antidepressant without psychotomimetic side effects. *Transl. Psychiatry* **2015**, *5*, No. e632.

- (45) Ethell, I. M.; Pasquale, E. B. Molecular Mechanisms of Dendritic Spine Development and Remodeling. *Prog. Neurobiol.* **2005**, *75*, 161–205.
- (46) Swanger, S. A.; Mattheyes, A. L.; Gentry, E. G.; Herskowitz, J. H. ROCK1 and ROCK2 Inhibition Alters Dendritic Spine Morphology in Hippocampal Neurons. *Cell. Logist.* **2015**, *5* (4), No. e113266.
- (47) Meerson, A.; Cacheaux, L.; Goosens, K. A.; Sapolsky, R. M.; Soreq, H.; Kaufer, D. Changes in Brain MicroRNAs Contribute to Cholinergic Stress Reactions. *J. Mol. Neurosci.* **2010**, *40*, 47–55.
- (48) Schratt, G. MicroRNAs at the Synapse. *Nat. Rev. Neurosci.* **2009**, *10*, 842–849.
- (49) Safa, A.; Abak, A.; Shoorei, H.; Taheri, M.; Ghafouri-Fard, S. MicroRNAs as Regulators of ERK/MAPK Pathway: A Comprehensive Review. *Biomed. Pharmacother.* **2020**, *132*, 110853.
- (50) Gao, J.; Wang, W.-Y.; Mao, Y.-W.; Gräff, J.; Guan, J.-S.; Pan, L.; Mak, G.; Kim, D.; Su, S. C.; Tsai, L.-H. A Novel Pathway Regulates Memory and Plasticity via SIRT1 and MiR-134. *Nature* **2010**, *466*, 1105–1109.
- (51) Bicker, S.; Lackinger, M.; Weiß, K.; Schratt, G. MicroRNA-132, -134, and -138: A MicroRNA Troika Rules in Neuronal Dendrites. *Cell. Mol. Life Sci.* **2014**, *71*, 3987–4005.
- (52) Siegel, G.; Obernosterer, G.; Fiore, R.; Oehmen, M.; Bicker, S.; Christensen, M.; Khudayberdiev, S.; Leuschner, P. F.; Busch, C. J. L.; Kane, C.; Hübel, K.; Dekker, F.; Hedberg, C.; Rengarajan, B.; Drepper, C.; Waldmann, H.; Kauppinen, S.; Greenberg, M. E.; Draguhn, A.; Rehmsmeier, M.; Martinez, J.; Schratt, G. M. A Functional Screen Implicates MicroRNA-138-Dependent Regulation of the Depalmitoylation Enzyme APT1 in Dendritic Spine Morphogenesis. *Nat. Cell Biol.* **2009**, *11* (6), 705–716.
- (53) Shen, Z. C.; Xia, Z. X.; Liu, J. M.; Zheng, J. Y.; Luo, Y. F.; Yang, H.; Li, M. D.; Cao, T.; Liu, H. P.; Jin, G. L.; Huang, H. H.; Yu, C. X.; Zhou, J. APT1-Mediated Depalmitoylation Regulates Hippocampal Synaptic Plasticity. *J. Neurosci.* **2022**, *42* (13), 2662–2677.
- (54) Gu, J.; Li, Y.; Tian, Y.; Zhang, Y.; Cheng, Y.; Tang, Y. Noncanonical Functions of MicroRNAs in the Nucleus. *Acta Biochim. Biophys. Sin.* **2024**, *56*, 151–161.
- (55) Boran, A. D. W.; Iyengar, R. Systems Pharmacology. *Mt. Sinai J. Med.* **2010**, *77*, 333–344.
- (56) Ji, H.; Tucker, K. R.; Putzier, I.; Huertas, M. A.; Horn, J. P.; Canavier, C. C.; Levitan, E. S.; Shepard, P. D. Functional Characterization of Ether-à-Go-Go-Related Gene Potassium Channels in Midbrain Dopamine Neurons - Implications for a Role in Depolarization Block. *Eur. J. Neurosci.* **2012**, *36* (7), 2906–2916.
- (57) Atalar, F.; Acuner, T. T.; Cine, N.; Oncu, F.; Yesilbursa, D.; Ozbek, U.; Turkcan, S. Two Four-Marker Haplotypes on 7q36.1 Region Indicate That the Potassium Channel Gene HERG1 (KCNH2, Kv11.1) Is Related to Schizophrenia: A Case Control Study. *Behav. Brain Funct.* **2010**, *6*, 27.
- (58) Imbrici, P.; Camerino, D. C.; Tricarico, D. Major Channels Involved in Neuropsychiatric Disorders and Therapeutic Perspectives. *Front. Genet.* **2013**, *4* (MAY), 76.
- (59) Lee, H. A.; Kim, K. S.; Hyun, S. A.; Park, S. G.; Kim, S. J. Wide Spectrum of Inhibitory Effects of Sertraline on Cardiac Ion Channels. *Korean J. Physiol. Pharmacol.* **2012**, *16* (5), 327–332.
- (60) Alvarez, P.; Pahissa, J. QT Alterations in Psychopharmacology: Proven Candidates and Suspects. *Curr. Drug Saf.* **2010**, *5*, 97–104.
- (61) Ray, P.; Wright, J.; Adam, J.; Bennett, J.; Boucharens, S.; Black, D.; Cook, A.; Brown, A. R.; Epemolu, O.; Fletcher, D.; Haunso, A.; Huggett, M.; Jones, P.; Laats, S.; Lyons, A.; Mestres, J.; De Man, J.; Morphy, R.; Rankovic, Z.; Sherborne, B.; Sherry, L.; Van Straten, N.; Westwood, P.; Zaman, G. Z. R. Fragment-Based Discovery of 6-Substituted Isoquinolin-1-Amine Based ROCK-I Inhibitors. *Bioorg. Med. Chem. Lett.* **2011**, *21* (1), 97–101.
- (62) Jiang, L.; Liu, X.; Kolokythas, A.; Yu, J.; Wang, A.; Heidbreder, C. E.; Shi, F.; Zhou, X. Downregulation of the Rho GTPase Signaling Pathway Is Involved in the MicroRNA-138-Mediated Inhibition of Cell Migration and Invasion in Tongue Squamous Cell Carcinoma. *Int. J. Cancer* **2010**, *127* (3), 505–512.
- (63) Fan, X.; Sun, L.; Qin, Y.; Liu, Y.; Wu, S.; Du, L. The Role of HSP90 Molecular Chaperones in Depression: Potential Mechanisms. *Mol. Neurobiol.* **2024**, *62*, 708–717.
- (64) Sabbagh, J. J.; Cordova, R. A.; Zheng, D.; Criado-Marrero, M.; Lemus, A.; Li, P.; Baker, J. D.; Nordhues, B. A.; Darling, A. L.; Martinez-Licha, C.; Rutz, D. A.; Patel, S.; Buchner, J.; Leahy, J. W.; Koren, J.; Dickey, C. A.; Blair, L. J. Targeting the FKBPS1/GR/Hsp90 Complex to Identify Functionally Relevant Treatments for Depression and PTSD. *ACS Chem. Biol.* **2018**, *13* (8), 2288–2299.
- (65) Banach, E.; Szczepankiewicz, A.; Leszczynska-Rodziewicz, A.; Pawlak, J.; Dmitrzak-Weglarcz, M.; Zaremba, D.; Twarowska-Hauser, J. Venlafaxine and Sertraline Does Not Affect the Expression of Genes Regulating Stress Response in Female MDD Patients. *Psychiatr. Pol.* **2017**, *51* (6), 1029–1038.
- (66) Liu, R.; Dang, W.; Jianting, M.; Su, C.; Wang, H.; Chen, Y.; Tan, Q. Citalopram Alleviates Chronic Stress Induced Depression-like Behaviors in Rats by Activating GSK3 β Signaling in Dorsal Hippocampus. *Brain Res.* **2012**, *1467*, 10–17.
- (67) Joaquim, H. P. G.; Talib, L. L.; Forlenza, O. V.; Diniz, B. S.; Gattaz, W. F. Long-Term Sertraline Treatment Increases Expression and Decreases Phosphorylation of Glycogen Synthase Kinase-3B in Platelets of Patients with Late-Life Major Depression. *J. Psychiatr. Res.* **2012**, *46* (8), 1053–1058.
- (68) Quesseveur, G.; Repérant, C.; David, D. J.; Gardier, A. M.; Sanchez, C.; Guiard, B. P. 5-HT2A Receptor Inactivation Potentiates the Acute Antidepressant-like Activity of Escitalopram: Involvement of the Noradrenergic System. *Exp. Brain Res.* **2013**, *226* (2), 285–295.
- (69) Yang, Z.; Jiang, Y.; Xiao, Y.; Qian, L.; Jiang, Y.; Hu, Y.; Liu, X. Di-Huang-Yin-Zi Regulates P53/SLC7A11 Signaling Pathway to Improve the Mechanism of Post-Stroke Depression. *J. Ethnopharmacol.* **2024**, *319*, 117226.
- (70) Zhang, G.; Lv, S.; Zhong, X.; Li, X.; Yi, Y.; Lu, Y.; Yan, W.; Li, J.; Teng, J. Ferroptosis: A New Antidepressant Pharmacological Mechanism. *Front. Pharmacol.* **2024**, *14*, 1339057.
- (71) Morton, D.; Griffiths, P. Guidelines on the Recognition of Pain, Distress and Discomfort in Experimental Animals and an Hypothesis for Assessment. *Vet. Rec.* **1985**, *116* (16), 431–436.
- (72) Wu, J.; Li, J.; Hu, H.; Liu, P.; Fang, Y.; Wu, D. Rho-Kinase Inhibitor, Fasudil, Prevents Neuronal Apoptosis via the Akt Activation and Pten Inactivation in the Ischemic Penumbra of Rat Brain. *Cell. Mol. Neurobiol.* **2012**, *32* (7), 1187–1197.
- (73) Song, Y.; Chen, X.; Wang, L. Y.; Gao, W.; Zhu, M. J. Rho Kinase Inhibitor Fasudil Protects against β -Amyloid-Induced Hippocampal Neurodegeneration in Rats. *CNS Neurosci. Ther.* **2013**, *19* (8), 603–610.
- (74) Wei, X.-E.; Zhang, F.-Y.; Wang, K.; Zhang, Q.-X.; Rong, L.-Q. Fasudil Hydrochloride Protects Neurons in Rat Hippocampal CA1 Region through Inhibiting GluR6–MLK3–JNKs Signal Pathway. *Cell Biochem. Biophys.* **2014**, *70* (1), 415–421.
- (75) Mendez, D.; Gaulton, A.; Bento, A. P.; Chambers, J.; De Veij, M.; Félix, E.; Magariños, M.; Mosquera, J. F.; Mutowo, P.; Nowotka, M.; Gordillo-Marañón, M.; Hunter, F.; Junco, L.; Mugumbate, G.; Rodriguez-Lopez, M.; Atkinson, F.; Bosc, N.; Radoux, C. J.; Segura-Cabrera, A.; Hersey, A.; Leach, A. R. ChEMBL: Towards Direct Deposition of Bioassay Data. *Nucleic Acids Res.* **2019**, *47* (D1), D930–D940.
- (76) Bento, A. P.; Gaulton, A.; Hersey, A.; Bellis, L. J.; Chambers, J.; Davies, M.; Krüger, F. A.; Light, Y.; Mak, L.; McGlinchey, S.; Nowotka, M.; Papadatos, G.; Santos, R.; Overington, J. P. The ChEMBL Bioactivity Database: An Update. *Nucleic Acids Res.* **2014**, *42* (D1), D1083–D1090.
- (77) Sheils, T. K.; Mathias, S. L.; Kelleher, K. J.; Siramshetty, V. B.; Nguyen, D. T.; Bologa, C. G.; Jensen, L. J.; Vidović, D.; Koleti, A.; Schürer, S. C.; Waller, A.; Yang, J. J.; Holmes, J.; Bocci, G.; Southall, N.; Dharkar, P.; Mathé, E.; Simeonov, A.; Oprea, T. I. TCRD and Pharos 2021: Mining the Human Proteome for Disease Biology. *Nucleic Acids Res.* **2021**, *49* (D1), D1334–D1346.

(78) Szklarczyk, D.; Kirsch, R.; Koutrouli, M.; Nastou, K.; Mehryary, F.; Hachilif, R.; Gable, A. L.; Fang, T.; Doncheva, N. T.; Pyysalo, S.; Bork, P.; Jensen, L. J.; von Mering, C. The STRING Database in 2023: Protein-Protein Association Networks and Functional Enrichment Analyses for Any Sequenced Genome of Interest. *Nucleic Acids Res.* **2023**, *S1* (D1), D638–D646.

(79) Hagberg, A. A.; Schult, D. A.; Swart, P. J. Exploring Network Structure, Dynamics, and Function Using NetworkX. In *7th Python in Science Conference (SciPy 2008)*, 2008.

(80) Ochoa, D.; Hercules, A.; Carmona, M.; Suveges, D.; Gonzalez-Uriarte, A.; Malangone, C.; Miranda, A.; Fumis, L.; Carvalho-Silva, D.; Spitzer, M.; Baker, J.; Ferrer, J.; Raies, A.; Razuvayevskaya, O.; Faulconbridge, A.; Petsalaki, E.; Mutowo, P.; MacHlitt-Northen, S.; Peat, G.; McAuley, E.; Ong, C. K.; Mountjoy, E.; Ghousaini, M.; Pierleoni, A.; Papa, E.; Pignatelli, M.; Koscielny, G.; Karim, M.; Schwartzentruber, J.; Hulcoop, D. G.; Dunham, I.; McDonagh, E. M. Open Targets Platform: Supporting Systematic Drug-Target Identification and Prioritisation. *Nucleic Acids Res.* **2021**, *49* (D1), D1302–D1310.

(81) Arikath, J. Molecular Mechanisms of Dendrite Morphogenesis. *Front. Cell. Neurosci.* **2012**, *6*, 61.

(82) Huang, H. Y.; Lin, Y. C. D.; Cui, S.; Huang, Y.; Tang, Y.; Xu, J.; Bao, J.; Li, Y.; Wen, J.; Zuo, H.; Wang, W.; Li, J.; Ni, J.; Ruan, Y.; Li, L.; Chen, Y.; Xie, Y.; Zhu, Z.; Cai, X.; Chen, X.; Yao, L.; Chen, Y.; Luo, Y.; Luxu, S.; Luo, M.; Chiu, C. M.; Ma, K.; Zhu, L.; Cheng, G. J.; Bai, C.; Chiang, Y. C.; Wang, L.; Wei, F.; Lee, T. Y.; Huang, H. Da. MiRTarBase Update 2022: An Informative Resource for Experimentally Validated MiRNA-Target Interactions. *Nucleic Acids Res.* **2022**, *S0* (1), D222–D230.